

NISTIR 7094

Structural Collapse Fire Tests: Single Story, Wood Frame Structures

David W. Stroup
Nelson P. Bryner
Jack Lee
Jay McElroy
Gary Roadarmel
William H. Twilley



FEMA

Sponsored in part by
Department of Homeland Security
Federal Emergency Management Agency
United States Fire Administration

NIST

National Institute of Standards and Technology
Technology Administration, U.S. Department of Commerce

NISTIR 7094

Structural Collapse Fire Tests: Single Story, Wood Frame Structures

David W. Stroup
Nelson P. Bryner
Jack Lee
Jay McElroy
Gary Roadarmel
William H. Twilley
*Fire Research Division
Building and Fire Research Laboratory
National Institute of Standards and Technology
Gaithersburg, MD 20899-8661*

March 2004



Department of Homeland Security
Tom Ridge, Secretary
Federal Emergency Management Agency
*Michael D. Brown, Under Secretary of Emergency
Preparedness and Response*
United States Fire Administration
R. David Paulison, Administrator



U.S. Department of Commerce
Donald L. Evans, Secretary
Technology Administration
Phillip J. Bond, Under Secretary for Technology
National Institute of Standards and Technology
Arden L. Bement, Jr., Director

Table of Contents

	<u>Page</u>
Abstract.....	1
Introduction.....	1
Experimental Configuration.....	3
Experiments	6
Full Scale Fire Tests.....	6
Cone Calorimeter Experiments.....	8
Results.....	9
Full Scale Fire Tests.....	9
Temperature Data.....	9
Infrared Camera Data.....	11
Cone Calorimeter Experiments.....	13
Uncertainty Analysis.....	14
Conclusions.....	16
Acknowledgements.....	17
References.....	17
Appendix A – Cone Calorimeter Test Data.....	67

List of Figures

		<u>Page</u>
Figure 1.	Photograph showing the front and one side of test structure with tile roof prior to start of test.....	20
Figure 2.	Photograph showing rear and one side of test structure with asphalt single roof prior to start of test	21
Figure 3.	Plan view of test structure showing approximate placement of furniture and other items within structure (not to scale).....	22
Figure 4.	Plan view of test structure showing locations of measurement instruments and dimensions (all dimensions in m)	23
Figure 5.	Diagram showing typical construction of the test structure.....	24
Figure 6.	Photograph showing living room ceiling with ceiling louvers, electrical boxes, and attic access	25
Figure 7.	Photograph of living room area showing furniture arrangement.....	26
Figure 8.	Photograph showing living room with furniture, cabinets, and thermocouple array	27
Figure 9.	Photograph showing furniture in bedroom area of test structure (thermocouple array is visible in the foreground.).....	28
Figure 10.	Photograph showing two double beds, night tables and lamps in the bedroom	29
Figure 11.	Photograph showing trusses supporting the roof structure with thermocouple array visible in front of second vertical wood member	30
Figure 12.	Photograph of living room showing ignition location in corner of couch under newspaper	31
Figure 13.	Photograph showing bedroom with ignition location in corner of chair under the newspaper	32
Figure 14.	Photograph of test structure at 60 s after ignition.....	33
Figure 15.	Photograph of test structure at 75 s after ignition.....	34
Figure 16.	Photograph of test structure at 120 s after ignition.....	35
Figure 17.	Photograph of test structure at 180 s after ignition.....	36
Figure 18.	Photograph of test structure at 210 s after ignition.....	37
Figure 19.	Photograph of test structure at 540 s after ignition.....	38
Figure 20.	Photograph of test structure at 640 s after ignition.....	39
Figure 21.	Photograph of test structure at 900 s after ignition when front door has burned away	40
Figure 22.	Photograph of test structure at 960 s after ignition with portion of roof structure burning	41
Figure 23.	Photograph of test structure at 1010 s after ignition as collapse is starting.....	42
Figure 24.	Photograph of test structure at 1140 s after ignition when suppression has been completed	43
Figure 25.	Schematic drawing of the cone calorimeter.....	44
Figure 26.	Graph showing temperatures measured in the living room during the first test (distances measured from ceiling downward).....	45

Figure 27.	Graph showing temperatures measured in the bedroom during the first test (distances measured from ceiling downward)	46
Figure 28.	Graph showing temperatures measured in the north portion of the attic during the first test (distances measured from roof peak downward).....	47
Figure 29.	Graph showing temperatures measured in the south portion of the attic during the first test (distances measured from roof peak downward).....	48
Figure 30.	Graph showing temperatures measured on the roof under the fire fighter mannequins' boots during the first test.....	49
Figure 31.	Graph showing temperatures measured in the living room during the second test (distances measured from ceiling downward).....	50
Figure 32.	Graph showing temperatures measured in the bedroom during the second test (distances measured from ceiling downward).....	51
Figure 33.	Graph showing temperatures measured in the north portion of the attic during the second test (distances measured from roof peak downward).....	52
Figure 34.	Graph showing temperatures measured in the south portion of the attic during the second test (distances measured from roof peak downward).....	53
Figure 35.	Graph showing temperatures measured on the roof under the fire fighter mannequins' boots during the second test	54
Figure 36.	Graph showing temperatures measured in the living room during the third test (distances measured from ceiling downward).....	55
Figure 37.	Graph showing temperatures measured in the bedroom during the third test (distances measured from ceiling downward).....	56
Figure 38.	Graph showing temperatures measured in the north portion of the attic during the third test (distances measured from roof peak downward).....	57
Figure 39.	Graph showing temperatures measured in the south portion of the attic during the third test (distances measured from roof peak downward).....	58
Figure 40.	Graph showing temperatures measured on the roof under the fire fighter mannequins' boots during the third test.....	59
Figure 41.	Graph showing temperatures measured in the living room during the fourth test (distances measured from ceiling downward).....	60
Figure 42.	Graph showing temperatures measured in the bedroom during the fourth test (distances measured from ceiling downward).....	61
Figure 43.	Graph showing temperatures measured in the north portion of the attic during the fourth test (distances measured from roof peak downward)	62
Figure 44.	Graph showing temperatures measured in the south portion of the attic during the fourth test (distances measured from roof peak downward)	63
Figure 45.	Graph showing temperatures measured on the roof under the fire fighter mannequins' boots during the fourth test.....	64
Figure 46.	Test 3 shown a few seconds after ignition (top – normal video, middle – Infrared Camera A, bottom – Infrared Camera B).....	65
Figure 47.	Test 3 shown approximately 10 s before collapse of the roof structure (top – normal video, middle Infrared Camera A, bottom – Infrared Camera B)	66

List of Tables

	<u>Page</u>
Table 1. Fuel Load	5
Table 2. Summary of Cone Calorimeter Data.....	14
Table 3. Uncertainty in Experimental Data	15

Structural Collapse Fire Tests: Single Story Wood Frame Structures

David W. Stroup, Nelson P. Bryner, Jack Lee,
Jay McElroy, Gary Roadarmel, and William H. Twilley

Abstract

A series of fire tests was conducted in Phoenix, Arizona to collect data for a project examining the feasibility of predicting structural collapse. The fire test scenario was selected as part of a training video being prepared by the Phoenix, Arizona Fire Department. Multiple fires were started in each structure to facilitate collapse; the fires were not intended to test the fire endurance of the structures. Four structures with different roof constructions were used for the fire tests. Temperatures were measured as a function of time in four locations within each structure. Furniture items were placed in the front and back of each structure to simulate living room and bedroom areas. The living room and bedroom areas of each structure were ignited simultaneously using electric matches. Peak temperatures obtained during the tests ranged from approximately 800 °C (1500 °F) to 1000 °C (1800 °F). The roof of each structure collapsed approximately 17 minutes after ignition. In addition to the full scale tests, the plywood and oriented strand board (OSB) roofing materials were tested using a cone calorimeter to characterize the fire properties of the materials.

Key Words:

building collapse; building fires; fire data; fire fighting; large scale fire tests; structural failure; temperature measurements

Introduction

Every year, approximately 100 fire fighters die in the line of duty, and 90,000 to 100,000 are injured [1]. In 1999, the United States Fire Administration estimated that slightly more than 30 % of the fire fighter fatalities occurring on the fire ground resulted from something other than stress and heart attacks [2]. Stress and heart attacks, accounting for almost half of the fire fighter fatalities, remain the leading cause of death. The categorization of the statistics does not lend itself to easy identification of those deaths that occurred due to structural issues including failure and collapse. Examination of specific incidents in 1999 indicates that 18 fire fighters or 16 % died as a result of being trapped in a structure or involved in a collapse [2]. Based on data obtained from 1979 through 1988, a report prepared by the National Fire Protection Association (NFPA) for the Federal Emergency Management Agency [3] indicates that 93 of the 474 fire fighters who were killed at structure fires died as a result of structural collapse. Of these, 60 % were caught or trapped in the collapse while 40 % were struck by collapsing walls or sections of walls. A subsequent report examined 1150 fire fighter fatalities that occurred during the period from 1983 through 1992 [4]. Of the 390 deaths that occurred at structure fires, 45 fire fighters

died as a result of being caught or trapped and 26 fire fighters were struck and killed by debris from the collapse. In a 2002 report [5], Dr. Fahy of NFPA indicates that the rate of deaths due to heart attacks at structural fire is decreasing while the rate of deaths due to traumatic injuries is increasing. Structural collapse is identified as one of the major causes of these traumatic injuries. A recent National Institute of Standards and Technology (NIST) report [6] indicates that deaths resulting from structural collapse have decreased overall during the last 23 years. However, the percentage of those deaths occurring at residential fires has been increasing.

As part of a project funded by the United States Fire Administration, the Building and Fire Research Laboratory (BFRL) at NIST is exploring the feasibility of developing a system for use by fire fighters to predict structural collapse during fire ground operations. Predicting a potential structural collapse is one of the most challenging tasks facing an incident commander at a fire scene. Usually the lack of information on the construction of the building, fire size, fire location, fire burn time, condition of the building, fuel load, etc., makes the task nearly impossible.

The fire department in the City of Phoenix, Arizona conducted a series of live fire training exercises in various structures in an effort to better educate fire fighters about structural collapse. While some of the structures in this ongoing series of training exercises were scheduled for demolition [7], other structures such as those described in this report were built specifically for the fire tests. Each structure was allowed to burn until some portion of the structure collapsed. In collaboration with the Phoenix Fire Department, researchers from NIST provided measurement support during the fire tests. Using video and data obtained from two different fire test series, the fire department developed a set of three videotapes dealing with fire ground command and collapse issues [8].

This report presents the results obtained from a set of tests that were conducted in single story wood frame residential structures. These structures were constructed for test experiments in order to examine several issues related to fire fighter health and safety. The first goal of the tests was to obtain temperature data from a burning structure during a collapse. Second, various techniques and tools were being evaluated for use in predicting structural collapse. Specifically, the use of thermal imaging techniques was being examined as a means to predict collapse. In addition, the exterior of the building was observed prior to and during collapse to identify any visual indicators of impending collapse. Subsequent reports will provide additional analysis of these fires and will also assess the effectiveness of various methodologies for predicting the onset of structural collapse.

These tests were not designed to evaluate the fire endurance of wood trusses, gypsum wallboard, wood studs, or any other structural elements used in the construction of the four structures. The fire scenario used in this study was designed to reach flashover conditions rapidly to force a partial or complete collapse of the structure. Many factors influence the failure of structural elements including the load on the element, protection of the element, fire intensity, and fire duration. More or less time may be available before failure of the element depending on the particular fire scenario. Kenneth E. Bland provides a review of and expert procedure for predicting the failure of wood assemblies when exposed to fire [9]. Using the Component

Additive Method (CAM) procedures presented in his report, the fire resistance rating of a wood roof assembly consisting of wood trusses, spaced 0.6 m (24 in) on center and protected by a 12.7 mm (½ in) thick layer of gypsum board would be at least 20 min. The CAM procedures assume the gypsum board is continuous, unlike the Phoenix fire tests where an attic access hole was located directly above the couch.

The fire resistance and ability of a structural member to maintain its load during an actual fire are influenced by a number of factors. Many of these factors can vary significantly depending on the specific fire scenario. Fire resistance ratings and measured or predicted times to failure or collapse should not be relied upon as absolute indicators of time available for operating on or within a burning structure. Each structure must be evaluated and reevaluated during the fire to determine whether or not it is safe for fire fighters to remain within any potential collapse zone.

Experimental Configuration

The Phoenix Fire Department built four single story wood frame residential type structures for this series of tests. These structures were identical except for the roof construction. One structure had a roof consisting of asphalt shingles on 12.7 mm (½ in) five-ply plywood while a second structure had asphalt shingles on 12.7 mm (½ in) oriented strand board (OSB). Both structures had a layer of 6.8 kg (15 lb) felt paper between the asphalt shingles and the plywood or OSB. The other two structures used tile over either plywood or OSB as the roof construction. The cementitious tile roofs had two layers of 13.6 kg (30 lb) felt over the plywood or OSB and nominally 25.4 mm (1 in) by 50.8 mm (2 in) boards to hold the tile in place. The measurements for the materials used to construct the test structures described in this report are approximate nominal dimensions.

Each structure consisted of two rooms and an attic space. The rooms were separated by a wall constructed of 2 x 4 wood studs with a layer of 12.7 mm (½ in) gypsum board nailed to each side. There was a doorway, 0.8 m (2.9 ft) wide and 2 m (6.5 ft) high, in the wall between the two rooms with its centerline located 4.5 m (14.9 ft) from one exterior wall and 0.7 m (2.4 ft) from the other exterior wall. Figure 1 is a photograph of the front of one of the structures, and Figure 2 provides a rear view. A typical structure is shown in plan view in Figure 3. The placement of the measurement instruments and dimensions of the structure are shown in Figure 4.

The exterior walls of the structures were composed of 2 x 4 wood studs on 0.4 m (1.3 ft) centers nailed to a single sole plate and a double top plate. The exterior surfaces of the walls were covered with 15.9 mm (5/8 in) T-1-11 wood siding using galvanized nails. Interior walls and ceilings had 12.7 mm (½ in) gypsum board nailed to the studs. All of the joints between boards were taped, and the taped joints and nails were covered with joint compound. In addition, the four walls in the back room (bedroom) and the two walls in the front room (living room) were covered with 3.2 mm (1/8 in) pressboard paneling attached using construction adhesive and small brads.

The front wall of the living room had a doorway, approximately 0.9 m (2.9 ft) wide and 2 m (6.7 ft) high, located with its centerline 0.6 m (1.9 ft) from one wall and 4.2 m (14.8 ft) from the opposite wall. A hollow core wood door was mounted in the doorway opening. In the living room of each structure, the walls adjacent to the front wall each had an approximately 1.2 m (4 ft) wide by 0.9 m (3ft) high section removed to let air into the room. One wall in the bedroom had a 1.2 m (4 ft) wide by 0.9 m (3 ft) high section removed, and the rear wall had a 0.9 m (3 ft) by 0.9 m (3 ft) window with glass. Each of the three cutout sections of wall had a piece of plywood on a slide track allowing it to be moved back and forth to regulate the flow of air into the room.

The roof system was built with manufactured trusses on 0.6 m (2 ft) centers (Figure 5). The gable ends were studded with 51 mm (2 in) by 76 mm (3 in) lumber and covered with 12.7 mm (½ in) high density fiberboard. The trusses were nailed on each end and attached to the top plate with metal hurricane ties. All structures had 2 x 6 boards nailed to the truss tails and the tails on the trusses were cut off at 0.5 m (1.7 ft). The outside rafts were nailed to 2 x 4 boards and attached to the second truss at 1.2 m (4 ft) intervals.

A 1.5 m (5 ft) long base cabinet made of particle board and a counter top were placed along the front wall of the living room. A second 1.5 m (5 ft) long cabinet was nailed to the wall above the first cabinet. Electrical outlet boxes were installed in the walls at various locations throughout the two rooms. A 0.3 m (0.8 ft) by 0.3 m (0.8 ft) hole was cut in the center of the ceiling in the living room and covered with a plastic grill to simulate a vent. The location of this vent was selected to facilitate fire spread into the attic space. A 0.6 m (2 ft) by 0.8 m (2.5 ft) hole was cut in the ceiling of the living room to allow access to the attic space. This opening was covered with a 12.7 mm (½ in) piece of drywall held in place using wood molding strips (Figure 6).

Identical pieces of furniture, typical of a residential occupancy, were placed in each of the four structures. The living room contained a couch, a love seat, and two chairs consisting of wood frames with polyurethane foam cushioning material. Two wood end tables, a wood coffee table, and two table lamps were also placed in the living room (Figures 7 and 8). The bedroom contained two sets of foam mattresses and box springs on metal frames. Wood bed tables were placed adjacent to each bed. Two wood dressers were located in the room. One dresser was located along the wall opposite the ends of the two beds while the second dresser was adjacent to the side of the second bed. Finally, a chair with polyurethane padding on a wood frame was positioned in the bedroom diagonally opposite the end corner of the first bed (Figures 9 and 10). Table lamps were placed on top of the two bed tables. The mass of each object in the two rooms for all four tests is summarized in Table 1. Both rooms in each structure had nylon wall-to-wall carpet laid on the floor over 1.4 kg (3 lb) pad.

Table 1. Fuel Load

Item	Test No. 1 Weight kg (lb)	Test No. 2 Weight kg (lb)	Test No. 3 Weight kg (lb)	Test No. 4 Weight kg (lb)
Bedroom				
Chair	34 (75)	32.7 (72)	30.8 (68)	34.5 (76)
Dresser 1	50.8 (112)	45.3 (100)	49 (108)	47.6 (105)
Bed Stand 1	13.6 (30)	13.6 (30)	13.6 (30)	13.6 (30)
Lamp 1	4.5 (10)	3.6 (8)	2.7 (6)	2.3 (5)
Bed 1	64.9 (143)	63.5 (140)	64 (141)	64.4 (142)
Bed Stand 2	9.5 (21)	14 (31)	13.6 (30)	13.6 (30)
Lamp 2	4 (9)	2.3 (5)	2.7 (6)	3.2 (7)
Bed 2	69.9 (154)	62.6 (138)	63.5 (140)	65.8 (145)
Dresser 2	50.3 (111)	45.3 (100)	50.8 (112)	49.4 (109)
Living Room				
Chair 1	35.4 (78)	36.3 (80)	34.5 (76)	35.8 (79)
Table Lamp 1	1.8 (4)	4.5 (10)	3.6 (8)	3.2 (7)
End Table 1	14 (31)	13.6 (30)	13.6 (30)	14 (31)
Sofa	97.5 (215)	98.9 (218)	87.5 (193)	95.3 (210)
Table Lamp 2	2.3 (5)	4.5 (10)	2.7 (6)	3.2 (7)
End Table 2	13.6 (30)	13.6 (30)	13.6 (30)	13.6 (30)
Chair 2	33.6 (74)	33.6 (74)	30.4 (67)	32.7 (72)
Coffee Table	19.1 (42)	20 (44)	21.8 (48)	20.4 (45)
Love Seat	51.7 (114)	51.7 (114)	51.3 (113)	50.8 (112)

Four thermocouple arrays were positioned in each structure to obtain temperature data during the fire test. The first array was located in the living room 0.8 m (2.6 ft) from the front wall and 0.8 m (2.6 ft) from the adjacent wall. The second thermocouple array was placed in the rear room between the two beds, 1.6 m (5.3 ft) from the rear wall and 2.6 m (8.6 ft) from the north wall. These arrays had Chromel-Alumel (Type K)¹ thermocouples located at 25 mm (1 in), 0.3 m (1 ft), 0.6 m (2 ft), 0.9 m (3 ft), 1.2 m (4 ft), 1.5 m (5 ft), 1.8 m (6 ft), and 2.1 m (7 ft) below the ceiling. Two thermocouple arrays were located in the attic space along the attic centerline that ran parallel to the front wall of each structure. These arrays were located 0.8 m (2.6 ft) from either gabled end of each structure. The attic arrays had thermocouples located at 25 mm (1 in), 0.2 m (0.5 ft), 0.3 m (1 ft), 0.5 m (1.5 ft), 0.6 m (2 ft), 0.8 m (2.5 ft), 0.9 m (3 ft), and 1.1 m (3.5 ft) below the attic peak (Figure 11).

¹ Certain commercial equipment, instruments, or materials are identified in this paper to foster understanding. Such identification does not imply recommendation or endorsement by the National Institute of Standards and Technology, nor does it imply that the materials or equipment identified are necessarily the best available for the purpose.

Two mannequins outfitted in fire fighter turnout gear with self-contained breathing apparatus were placed on the roof of each structure during the test. Each fire fighter mannequin had a mass of approximately 127 kg (280 lb) with gear, and they were positioned on the roof using metal stands. One fire fighter was placed in a bending position while the second stood upright (Figure 1). Thermocouples were located in contact with the roof surface under the left and right boot of each fire fighter mannequin. The tiles were removed from under the mannequins' boots for tests 3 and 4. A roof mounted air conditioning unit was also placed on the roof of each structure. Each air conditioning unit had an approximate mass of 227 kg (500 lb) and was placed on the sloped portion of the roof opposite the fire fighter mannequin locations.

Each test was documented using standard video, infrared cameras, and still photographs. Two separate infrared cameras monitoring different portions of the electromagnetic band were used during the tests. One of the infrared imagers, Camera A provided less quantitative temperature data, but was representative of infrared cameras typically used by fire departments. The other infrared imager, Camera B, provided significantly more resolution in temperature data, different measurement ranges, emissivity factors, adjustable sensing spans, and calibration capability, but it was not designed for fire fighter use. The video and infrared cameras were mounted on a fire department ladder truck. During each fire test, the ladder with the standard video and two infrared cameras was elevated to provide a similar overhead view of each structure for the three cameras.

Experiments

Full Scale Fire Tests

Two fires were ignited simultaneously in each structure using electric matches. Electric matches are matchbooks with a short length of Ni-Chrome wire wrapped around the match heads. When a small electric current passes through the wire, the wire heats up and ignites the matchbook. One electric match was placed in a slit in the couch in the front room and covered with paper towels and newspaper (Figure 12). A second electric match was positioned in a slit in the chair in the back room and covered with paper towels and newspaper (Figure 13).

The fires were ignited in each room simultaneously and allowed to grow to flashover. Flashover occurs when multiple combustible items in a room ignite as a result primarily of being heated by the intense thermal radiation from the hot upper layer. At flashover, the room environment is characterized as well stirred with temperatures throughout the space being relatively uniform. Gas temperatures in the room typically exceed 600 °C (1110 °F). During this test series, the fire ultimately spread into the attic space and eventually caused collapse of a portion of the roof structure. For this test series, collapse was assumed to occur when the portion of the roof supporting the fire fighter mannequins failed and allowed fire to envelope the mannequins. As the roof structure collapsed, the fire fighter mannequins were removed using a fire department crane. Once the mannequins were removed, the fire was extinguished using water or a

combination of water and a fire suppression foam agent. The test sequence is depicted in Figures 14 through 24.

Test No. 1 was conducted using the structure with a roof composed of asphalt shingles over plywood. For the first test, smoke became visible coming from the structure approximately 60 s after ignition. At approximately 3 min after ignition, the living room reached flashover temperatures. The bedroom reached flashover temperatures about 6 ½ min after ignition. After approximately 1 min, the temperatures in the living room dropped to a relatively uniform 500 °C (930 °F). The bedroom temperatures remained near 600 °C (1110 °F). The fire appears to have penetrated into the attic space at about 7 ½ min after ignition. At 14 min, portions of the roof began to burn. Collapse of a portion of the roof and removal of the firefighter mannequins occurred 17 ½ min after ignition. Fire suppression was initiated at 18 min 40 s.

Test No. 2 was conducted using the structure with a roof composed of asphalt shingles over oriented strand board. In the second test, smoke became visible coming from the structure approximately 52 seconds after ignition. At approximately 3 ½ min after ignition, the living room temperatures briefly exceeded flashover temperatures. Temperatures in the bedroom area never exceeded the 600 °C (1110 °F) flashover threshold until near the end of the test. The living room maintained peak temperatures in excess of 500 °C (930 °F) while the temperatures in the bedroom remained between 400 °C (750 °F) and 600 °C (1110 °F). The fire appears to have penetrated into the attic space at about 8 min after ignition. Flames began lapping the roof 13 min after ignition and the front door failed. At 14 min, portions of the roof began to burn. Collapse of a portion of the roof and removal of the firefighter mannequins occurred 17 min after ignition. Suppression was initiated at 17 min 45 s.

Test No. 3 was conducted using the structure with a roof composed of cementitious tile over plywood. During the third test, smoke became visible coming from the structure approximately 1 min 20 s after ignition. At approximately 3 min after ignition, the living room reached flashover temperatures of approximately 600 °C (1110 °F). The living room continued to maintain temperatures in excess of 600 °C (1110 °F) for most of the test period. Temperatures in the bedroom remained below flashover temperatures until 11 min after ignition. The fire appears to have penetrated into the attic space again at 8 min after ignition. Collapse of a portion of the roof and removal of the firefighter mannequins occurred 16 min after ignition. Suppression was initiated at 17 min. White smoke was observed coming from the structure at 19 min 40 s.

Test No. 4 was conducted using the structure with a roof composed of cementitious tile over oriented strand board. For the fourth test, smoke was first visible at approximately 56 s after ignition. Flashover temperatures were reached in the living room 4 min after ignition while the bedroom remained below flashover temperatures until almost 8 min after ignition. The fire penetrated into the attic space at about 8 min after ignition. Collapse of a portion of the roof and removal of the firefighter mannequins occurred 17 min 10 s after ignition. Suppression was initiated at 18 min.

Cone Calorimeter Experiments

The type of material, either plywood or OSB, which was used for the roofs of the structures is one of the variables examined during this study. In an effort to develop additional information about the materials and their response to fire exposure, samples were tested in the cone calorimeter. The cone calorimeter was developed at NIST in the 1980's [10], and it is presently the most commonly used bench-scale rate of heat release apparatus [11]. There are national [12] and international [13] standards documenting the apparatus and appropriate test procedures. Heat release rate is determined by the oxygen consumption method [14]. The gas flow rate in the exhaust duct is calculated from the pressure drop across and temperature at an orifice plate in the duct.

The cone calorimeter consists of a heater, spark ignitor, sample holder, and load cell located underneath an exhaust hood (Figure 25). Typically, the sample is located in the open with free access of air to the combustion zone. The heater consists of a 5-kW electrical heating element inside an insulated stainless-steel conical shell. Samples can be tested in either a horizontal or vertical orientation. When tests are performed in the horizontal configuration, the specimen is positioned approximately 25 mm (1 in) beneath the bottom plate of the cone heater. Flames and products of combustion pass through a circular opening at the top of the heater. The heater can expose samples to a maximum irradiance of approximately 100 kW/m².

For piloted ignition tests, an electric spark ignitor is positioned at the top of vertical samples and over the center of horizontal samples. Samples are typically 0.1 m (0.3 ft) by 0.1 m (0.3 ft), and they can be wrapped with aluminum foil to minimize edge effects. Combustion products and dilution air are extracted through the hood and exhaust duct by a high temperature fan. The flow rate can be adjusted between 0.01 m³/s (0.35 ft³/s) and 0.03 m³/s (1.1 ft³/s). The volumetric flow rate is maintained constant during testing. The sample is mounted on a load cell to determine mass loss rate during a test, and smoke obscuration is measured using a laser light source. Finally, the concentrations of carbon dioxide, carbon monoxide, and other gases are measured using appropriate instruments.

Three replicate tests of each sample were conducted at external heat fluxes of 35 kW/m² and 70 kW/m². For each test, the 0.1 m (0.3 ft) square sample was oriented horizontally under the cone heater. Data were recorded until approximately 20 % to 25 % of the original mass remained.

Results

Full Scale Fire Tests

Temperature Data

The temperature histories obtained for the first test are shown in Figures 26 through 30. As the fire in the living room grows to flashover, the stratified fire environment is evident from the distinct temperature histories obtained at the eight sampling locations (Figure 26). At about 200 s, the temperature plots indicate a “well stirred environment” with an average temperature of about 500 °C (930 °F). The fire in the bedroom takes longer to reach flashover temperatures; it reaches that point at about 420 s. At this point, the environment becomes well mixed with a temperature of about 600 °C (1100 °F) (Figure 27). Both the north (Figure 28) and south (Figure 29) thermocouple arrays in the attic indicate a stratified environment until about 700 s. The two peaks evident in both figures, one at about 180 s and the second at 200 s to 250 s, are most likely the result of periodic flame penetration into the attic space through the ceiling penetrations (Figure 6). At about 700 s, flashover appears to have occurred in the attic with the environment becoming well mixed at an average temperature of 750 to 800 °C (1380 to 1470 °F). The temperature plots suggest that some portions of the ceiling begin failing at about 800 s. In addition, the front door failed at about 840 s. The roof begins to collapse at 1050 s and suppression is started at 1120 s. The temperature data obtained on the roof surface beneath the fire fighter mannequin boots during the fire test is shown in Figure 30. Once flashover occurs in the attic at about 700 s, the temperatures under the boots increase rapidly to 800 °C (1470 °F), approximately the temperature within the attic space. Subsequently, the temperatures decrease correspondingly with decreasing temperatures within the attic space, possibly the result of failure of the ceiling. The temperatures gradually increase until roof collapse at which point the mannequins become surrounded by flames until their removal.

The temperature histories obtained for the second test are shown in Figures 31 through 35. In the living room, the fire grows to a temperature indicative of impending flashover, approximately 600 °C (1100 °F) within 180 s after ignition. After this initial period, the fire environment becomes stratified with a temperature gradient of 300 °C (570 °F) to 550 °C (1020 °F) for a period of about 180 s (Figure 31). At approximately 350 s after ignition, the entire living room area appears to flashover with a peak temperature of 700 °C (1300 °F). At this point, the environment in the living room becomes well mixed with a uniform temperature throughout most of the remainder of the test. The decrease in temperature occurring at approximately 400 s is the result of failure of some portion of the living room ceiling. After the fire begins spreading into the attic area, temperatures in the living room begin a steady climb to a peak of 1200 °C (2200 °F). The front door fails at about 840 s leading to a reduction in living room temperatures. Except for a few brief moments, the temperatures in the bedroom area never exceed 600 °C (1110 °F) (Figure 32). With the exception of the point at which the roof section collapsed at 1020 s, the environment in the bedroom remains stratified throughout the duration of the test. The first peak evident in Figures 33 and 34 at 180 s is most likely the result of flames

momentarily extending into the attic area through the ceiling ventilation louvers. A comparison of Figures 33 and 34 suggests that the attic access panel and possibly a portion of the ceiling near the ignition location failed at 400 s. The brief peak in Figure 34 at 725 s is probably the ignition of plastic light boxes in the ceiling. The attic area reaches a flashover condition at about 900 s. A portion of the roof under the fire fighter mannequins collapses approximately 4 min after flashover in the attic area. The temperature data obtained on the roof surface beneath the fire fighter mannequin boots during the fire test is shown in Figure 35. As the attic space approaches flashover conditions at about 800 s, the temperatures under the boots increase to 750 °C (1380 °F). At approximately 1020 s, the roof structure begins to collapse.

The temperature histories obtained for the third test are shown in Figures 36 through 40. As with the other tests, the temperatures in the living room rise rapidly at the start of the third test. At approximately 120 s, the space reaches temperatures indicative of flashover (Figure 36). After flashover, the environment becomes stratified with temperatures ranging from 300 °C (570 °F) to 600 °C (1110 °F). At about 550 s, the temperatures in the lower part of the living room increase producing an almost uniform environment of between 550 °C (1020 °F) and 600 °C (1110 °F). Just prior to a portion of the ceiling collapsing at about 700 s, the temperatures in the living room increase to about 700 °C (1290 °F). After collapse of a portion of the ceiling, the temperatures initially decrease then increase to 700 °C (1290 °F) to 800 °C (1470 °F). Collapse of a portion of the roof occurs at about 960 s. Prior to collapse of a portion of the ceiling, the bedroom temperatures remain well below 600 °C (1110 °F) (Figure 37). For the first 400 s of the test, the temperatures in both the north (Figure 38) and south (Figure 39) portions of the attic grow slowly to a peak of about 150 °C (300 °F). The temperature spikes during this period are indicative of flames momentarily extending into the attic area through the louvers and other ceiling penetrations (Figure 6). Once materials located in the attic start burning, the temperatures increase reaching a sustained maximum of 550 °C (1020 °F) with a momentary peak above 600 °C (1110 °F). When the roof collapses at 960 s, the attic temperatures initially increase then decrease rapidly as suppression is initiated. The temperatures under the fire fighter mannequins' boots remain close to ambient until the roof collapses at 960 s when the mannequins are enveloped in flame and removed (Figure 40).

The temperature histories obtained for the fourth test are shown in Figures 41 through 45. The temperature data obtained in the living room (Figure 41) indicates that the fire grew rapidly producing temperatures in excess of 600 °C (1110 °F). The environment in the living room remained at flashover temperatures and well mixed until about the time of roof collapse. The environment in the bedroom (Figure 42) remains stratified with a peak temperature of 420 °C (790 °F) until some portion of the ceiling fails at 450 s. After ceiling failure, the temperatures become somewhat erratic varying between 400 °C (750 °F) and almost 800 °C (1470 °F). At approximately 800 s, the temperatures in the bedroom become uniform and decrease then rapidly increase then decrease again. The most likely cause of this phenomenon is failure of additional portions of the ceiling as a result of flashover in the attic space. Temperature increase in both the north (Figure 43) and south (Figure 44) parts of the attic is relatively continuous with only slight discontinuities at about 450 s and 850 s. These discontinuities indicate ignition of materials in

the attic space and failure of the ceiling membrane between the living room/bedroom area and the attic. Once the attic space has flashed over at 900 s, the temperatures become uniform at approximately 750 °C (1380 °F) until collapse at 1030 s. The temperature data obtained on the roof surface beneath the fire fighter mannequin boots during the fire test is shown in Figure 45. Very little temperature increase is evident on the underside of the fire fighter boots until the roof collapses at 1030 s.

In all cases, some temperatures in the living room reach flashover temperatures (approximately 600 °C (1110 °F)) in at least some portion of the room within 180 s after ignition. With the exception of test 3, the living room temperatures remained at or above 600 °C (1110 °F) until roof collapse. Temperatures in excess of 600 °C (1110 °F) were seldom sustained in the bedroom until after apparent ignition of combustibles in the attic area. Combustible materials in the attic space appeared to ignite 400 s to 450 s after ignition during each test. With the exception of the first test, roof collapse appears to be preceded by flashover in the attic space. Even though the noncombustible tile was removed from beneath the fire fighter mannequins' boots, no temperature changes were measured under the boots until collapse of the roof during the third and fourth tests. The increased temperatures obtained during the first and second tests could be the result of burning of portions of the combustible roof structure remote from the mannequin locations.

Infrared Camera Data

Any substance will emit electromagnetic radiation as a result of electron motion associated with the internal energy of the material. This internal energy is a strong function of the temperature of the substance [15]. The emitted radiant energy can range from radio waves to cosmic rays. This radiant energy is always present, however, the human body can detect only a relatively small portion of it. Radiation that is detectable as heat or light is referred to as thermal radiation and occupies a wavelength range of 0.4 μm to 1000 μm .

The portion of this spectrum visible to the human eye is extremely small, ranging from 0.4 μm to approximately 0.7 μm . The color blue is in the range from 0.4 μm to 0.5 μm , the color green is in the range from 0.5 μm to 0.6 μm , and the color red is in the range from 0.6 μm to 0.7 μm . The infrared region of the spectrum is from 0.7 μm to 1000 μm . The infrared region of the spectrum is divided into three parts: near infrared, mid infrared, and thermal infrared. Only the thermal infrared portion, 3 μm to 1000 μm , is related to the sensation of heat. Infrared measurement devices typically operate somewhere in the range from 3 μm to approximately 30 μm .

Infrared thermometers have been in commercial use since the early 1960's. These electronic sensors capture the invisible infrared energy naturally emitted from all objects, in proportion to their temperature and material characteristics. The term emissivity is used to quantify the energy emitting characteristics of different materials. Most infrared temperature measuring devices include a user-adjustable emissivity to allow accurate measurement of different materials. An infrared camera or thermal imager package includes one or more lens, spectral filter detector,

processing electronics, and a housing to hold the components together and protect them from the environments. Some infrared imaging cameras measure temperature contours across a surface in front of the lens using scanning optics; other cameras use staring arrays to determine temperature contours. The total energy reaching the sensor is the sum of (1) energy emitted from the target, in proportion to temperature and emissivity; (2) energy reflected from the target, in proportion to its reflectivity or the presence of any hot objects nearby; and (3) energy transmitted through the target, in proportion to its transmissivity and the presence of any hot objects behind it. Emissivity and transmissivity are wavelength dependent properties for many materials.

Many factors enter into the considerations of the best camera waveband selection. The theoretical implications of operating in a particular waveband and the performance factors of the camera must be considered. Most infrared cameras are filtered to operate in the 3 μm to 5 μm and 8 μm to 14 μm waveband regions. These two operating regions are directly related to atmospheric propagation properties. If a wide range of applications is being considered, the 7 to 14 μm region would be preferred. However, more energy is available for detectors in the 3 to 5 μm region when the sources are very hot, 500 $^{\circ}\text{C}$ (930 $^{\circ}\text{F}$) to 1000 $^{\circ}\text{C}$ (1830 $^{\circ}\text{F}$).

During each fire test, two infrared cameras and one standard video camera were used to record similar views. Camera A, which was typical of what fire fighters might employ, utilizes focal plane array technology and is capable of detecting infrared radiation in the 8 to 14 μm range. Camera B, which is often used for research applications, operates using focal plane array technology and detects radiation in the waveband 3.4 to 5 μm . Camera B offers the user the ability to calibrate the focal plane array sensor, adjust the target emissivity, and achieve better temperature resolution by employing narrower temperature ranges. Camera B is capable of displaying quantitative temperature information, but also costs between three and five times more than Camera A. Figure 46 presents the same view from the three cameras a few seconds after ignition during test 3. The scene shown in Figure 47 is test 3 approximately 10 s prior to collapse of the roof structure. In both figures, the top image is from the standard video camera, the middle image is from Camera A, and the bottom image is from Camera B.

During these tests, the standard video camera documented that the roof began to sag or drop slightly just before failing completely. The time between the first appearance of a noticeable depression on the roof and the complete collapse of the roof appeared too short to allow any personnel on the roof to escape safely. The thermal images provided by the infrared cameras were also examined for evidence of an imminent collapse. The thermal images did not provide any warning of the roof collapse. The thermal radiation from the smoke plumes on both ends of the roof was radiated back to the surface of the roof. This reradiated energy appeared to wash out any thermal signature of the energy being conducted through the roof. Another factor that could make it difficult to see via thermal imager the energy being conducted through the roof would be the presence of water on the shingles or tiles. During one of the experiments, the fire department attempted to cool the boom of the extraction crane and the wind carried some of the water droplets onto one side of the roof. The temperature of the roof appeared to decrease, and the temperature difference across the wetted portion of the roof disappeared. The presence of hot smoke plumes or water from suppression activity or rain make it very difficult to see the thermal

signature of the fire through the roof. For this limited set of burn experiments, the thermal imagers did not appear to provide sufficient warning to allow fire fighters to escape before the roof collapsed.

Cone Calorimeter Experiments

Three replicate tests of each sample were conducted in the cone calorimeter. Each sample was exposed to either an external heat flux of 35 kW/m^2 or 70 kW/m^2 . Based on an analysis of heat flux data obtained by various researchers, Babrauskas recommends using a heat flux value of 35 kW/m^2 for materials exposed to pre-flashover fires [16]. For post flashover fire exposure, Babrauskas indicates potential heat fluxes as high as 150 kW/m^2 could be required. This value is beyond the capabilities of most laboratory scale apparatus including the cone calorimeter. In the post flashover fire data analyzed by Babrauskas, heat flux values for exposures to ceiling surfaces ranged from 67 to 147 kW/m^2 . In research by Madrzykowski [17], a value of 70 kW/m^2 is suggested as providing cone calorimeter results similar to full scale performance for certain materials.

For each test, the 0.1 m (0.3 ft) square sample was oriented horizontally under the cone heater. Each sample was wrapped in aluminum foil on all sides except for the exposed surface and placed in a metal frame. A number of flammability properties were measured including heat release rate, specimen mass loss rate, smoke generation rate, combustion gas production, and ignitability. The data obtained for each sample from the cone calorimeter tests is contained in Appendix A. The average values for each sample at the two external heat fluxes are shown in Table 2.

Table 2. Summary of Cone Calorimeter Data

Data Item	35 kW/m ²		70 kW/m ²	
	Plywood	OSB	Plywood	OSB
Peak Heat Release Rate (kW/m ²)	220	235	254	329
Time of Peak Heat Release Rate (s)	433	442	32	36
Average Heat Release Rate (kW/m ²)	115	156	168	223
Average Heat Release Rate at 60 s (kW/m ²)	123	165	164	267
Average Heat Release Rate at 180 s (kW/m ²)	93	156	157	231
Average Heat Release Rate at 300 s (kW/m ²)	95	142	180	231
Total Heat Released (MJ/m ²)	62	80	65	89
Average Effective Heat of Combustion (MJ/kg)	12.9	13.4	13.4	14.2
Average Specific Extinction Area (m ² /kg)	56	63.8	130.5	123.9
Average Mass Loss Rate (g/s/m ²)	9.9	12.1	14.4	16.9
Initial Specimen Mass (g)	64.7	76.4	64.0	79.5
Final Specimen Mass (g)	16.8	17.0	16.0	16.9
Average CO Yield (kg/kg)	0.0016	0.0023	0.00344	0.00391
Average CO ₂ Yield (kg/kg)	1.34	1.45	1.40	1.49
Time to Sustained Ignition (s)	47.1	39.7	7.7	10.6

As expected, the higher heat flux results in a more rapid ignition of both materials. It also leads to greater production of smoke and combustion gases. At the higher heat flux, the OSB has a peak heat release rate almost 100 kW greater than the peaks obtained from either material at 35 kW/m² and the plywood at 70 kW/m². The heat release rate for the OSB is approximately 100 kW greater than the other materials throughout the test at 70 kW/m². While the plywood mass was approximately 10 g less than the OSB at the start of each test, approximately the same mass of material remained at the end of the test. The total amount of energy liberated per square meter of material is significantly greater for the OSB than the plywood. The pyrolysis and combustion of the organic binder, which represents a higher mass fraction in OSB relative to plywood, would be consistent with a higher peak heat release rate.

Uncertainty Analysis

There are different components of uncertainty in the gas temperatures, mass of fuel packages, and time to collapse data reported here. Uncertainties are grouped into two categories according to the method used to estimate them. Type A uncertainties are those which are evaluated by statistical methods, and Type B are those which are evaluated by other means [18]. Type B analysis of systematic uncertainties involves estimating the upper (+ a) and lower (- a) limits for the quantity in question such that the probability that the value would be in the interval ($\pm a$) is essentially 100 %. After estimating uncertainties by either Type A or B analysis, the uncertainties are combined in quadrature to yield the combined standard uncertainty.

Multiplying the combined standard uncertainty by a coverage factor of two results in the expanded uncertainty which corresponds to a 95 percent confidence interval (2σ).

Components of uncertainty are tabulated in Table 3. Some of these components, such as the zero and calibration elements, are derived from instrument specifications, while other components, such as positioning include past experience. The combined standard uncertainty for gas temperature includes a component that is related to the position of the thermocouple. Each thermocouple array was carefully installed and positioned as each structure was prepared for each experimental burn. Each thermocouple was tested individually for proper response to flame temperatures. The position of each thermocouple was rechecked during the final steps prior to ignition. Several load cells were utilized to measure fuel package mass. Each load cell was calibrated with a standard mass prior to recording the mass of each fuel item. All fuel items, such as bed, dresser, or sofa, in a particular structure were weighed, then items were selected at random to be reweighed a second time in order to help estimate repeatability.

The combined standard uncertainty for infrared camera temperatures includes components related to the calibration of the thermal camera which were estimated from manufacturer specifications. Other uncertainty components including material emissivity and surface properties were estimated based on prior experience. Uncertainty components for the cone calorimeter were estimated based on manufacturer specifications and past experience using the cone calorimeter to collect ignition and flammability properties. Uncertainties associated with oxygen calorimetry techniques is discussed in greater detail by Babrabrauskas et al [19] and Bryant et al. [20]

Table 3. Uncertainty in Experimental Data

	Component Standard Uncertainty	Combined Standard Uncertainty	Total Expanded Uncertainty
Gas Temperature			
Zero	± 2 %		
Calibration	± 2 %		
Position	± 5 %	± 12 %	± 25 %
Repeatability	± 5 %		
Random	± 10 %		
Mass of Fuel Package			
Zero	± 2 %		
Calibration	± 7 %	± 9 %	± 18 %
Repeatability	± 5 %		
Random	± 3 %		

	Component Standard Uncertainty	Combined Standard Uncertainty	Total Expanded Uncertainty
Time to Collapse Repeatability Random	± 7 % ± 5 %	± 9 %	± 17 %
Infrared Camera Temperatures Zero Calibration Emissivity Repeatability Random	± 5 % ± 5 % ± 10 % ± 10 % ± 5 %	± 17 %	± 35 %
Cone Calorimeter Peak Heat Release Rate Time of Peak Heat Release Rate Average Heat Release Rate Total Heat Released Average Eff. Ht. of Combustion Average Specific Extinction Area Average Mass Loss Rate Specimen Mass Average CO Yield Average CO ₂ Yield Time to Sustained Ignition	± 13 % ± 4 % ± 10 % ± 14 % ± 10 % ± 10 % ± 10 % ± 10 % ± 5 % ± 10 % ± 10 % ± 5 %	± 13 % ± 4 % ± 10 % ± 14 % ± 10 % ± 10 % ± 10 % ± 10 % ± 5 % ± 10 % ± 10 % ± 5 %	± 25 % ± 8 % ± 20 % ± 28 % ± 20 % ± 20 % ± 20 % ± 20 % ± 10 % ± 20 % ± 20 % ± 10 %
Note: Random and repeatability evaluated as Type A, other components as Type B.			

Conclusions

For all four tests, the maximum temperatures in the living room and bedroom areas reached between 540 °C (1000 °F) and 815 °C (1500 °F). Flashover occurred in the living room spaces approximately 3 to 4 minutes after ignition. Prior to collapse, peak temperatures in the attic spaces were approximately 500 °C (930 °F). The fires broke through into the attic spaces between 6 minutes and 8 minutes after ignition. In all of the tests, collapse occurs approximately 17 minutes after ignition. Flashover in the attic spaces occurs approximately 5 ½ minutes after the fire breaks through the ceiling or 12 minutes after ignition. As the attic space approaches flashover, temperatures under the roof rapidly change (on the order of a few seconds) from near ambient 37 °C (100 °F) to 540 °C (1000 °F).

The temperature of the roof surface under the fire fighter mannequins' boots did not increase significantly prior to collapse. Temperature measurements obtained under fire fighter boots would probably not be a useful indicator of potential collapse. Unfortunately, the fire fighter mannequins did not move. Therefore, the influence of impact or dynamic loading from walking on the roof could not be evaluated. Impact loads on these roof structures could result in significantly less time to collapse.

Each of the roofs collapsed between approximately 16 ¾ min and 17 ½ min. This limited set of full-scale tests do not demonstrate significant difference between the performance of the plywood and OSB sheathing. No differences were observed between the asphalt shingles and the cementitious tiles. The other temperature data obtained during the tests did not indicate any difference in performance between the plywood and OSB. OSB releases energy faster and more of its total energy when exposed to high radiant heat fluxes in the cone calorimeter. While it is heat flux dependent, both materials ignite after about the same exposure time.

This limited set of burn tests indicated that infrared cameras may not be a viable tool for predicting structural collapse in residential structures. The thermal signature of the fire coming through the roof is washed out by radiation from smoke or fire plumes or was obscured by water spray or rain. Since one typically expects hot smoke or fire plumes as well as water sprays to be present at residential fire scenes, thermal images do not appear to be an adequate indicator of pending structural collapse.

Acknowledgements

The authors would like to thank the Phoenix Fire Department and Chief Alan Brunacini for inviting NIST to participate in this live fire training exercise. Captain Tom Bates of the Phoenix Fire Department deserves special recognition for the invaluable support that he provided to NIST staff during this test series. In addition, the authors are grateful to Mr. Michael Smith of the Building and Fire Research Laboratory at NIST for conducting the cone calorimeter tests. The authors would like to thank Mr. Francis L. Brannigan, author of Building Construction for the Fire Service, for providing comments on this report. Review of this document by the American Forest and Paper Association is also appreciated. Finally, the authors express gratitude to the United States Fire Administration and Mr. William Troup for their sponsorship and support of this important research.

References

- [1] Beyler, C.L., "Fire Safety Challenges in the 21st Century," Journal of Fire Protection Engineering, Vol. 11, No.1, pp. 4-15, 2001.
- [2] Fire Fighter Fatalities in the United States in 1999, United States Fire Administration, Emmitsburg, MD, July 2000.

- [3] "Fire Fighter Deaths in Structural Collapses, 1979-1988," National Fire Protection Association, Quincy, MA, August 1989.
- [4] "Fire Ground Fatalities as a Result of Structural Collapse, 1983-1992," National Fire Protection Association, Quincy, MA, August 1993.
- [5] Fahy, R.F., "U.S. Fire Service Fatalities in Structure Fires, 1977-2000," National Fire Protection Association, Quincy, MA, July 2002.
- [6] Brassell, L.D. and Evans, D.D., "Trends in Firefighter Fatalities Due to Structural Collapse, 1979-2002," NISTIR 7069, National Institute of Standards and Technology, Gaithersburg, MD, November 2003.
- [7] Stroup, D.W., Madrzykowski, D., Walton, W.D., and Twilley, W., "Structural Collapse Fire Tests: Single Story, Ordinary Construction Warehouse," NISTIR 6959, National Institute of Standards and Technology, Gaithersburg, MD, May 2003.
- [8] Brunacini, A., "Critical Fireground Factors Video Set," VCRSET1, National Fire Protection Association, Quincy, MA, 2002.
- [9] Bland, K.E., "Behavior of Wood Exposed to Fire: A Review and Expert Judgment Procedure for Predicting Assembly Failure," Master's Thesis, Worcester Polytechnic Institute, Worcester, MA, May 1994.
- [10] Babrauskas, V., "Development of the Cone Calorimeter – A Bench-Scale Heat Release Rate Apparatus Based on Oxygen Consumption," Journal of Fire and Materials, Vol. 8, pp. 81-95, 1984.
- [11] Janssens, M., "Section 3/Chapter 2: Calorimetry," The SFPE Handbook of Fire Protection Engineering, 2nd ed., SFPE, Bethesda, MD, pp. 3-16 – 3-36, 1995.
- [12] "ASTM E 1354: Test Method for Heat and Visible Smoke Release Rates for Materials and Products Using an Oxygen Consumption Calorimeter," ASTM Fire Test Standards, 4th ed., ASTM, Philadelphia, PA, pp. 968-984, 1993.
- [13] "ISO 5660-1: Rate of Heat Release of Building Products (Cone Calorimeter)," International Organization for Standardization, Geneva, Switzerland, 1992.
- [14] Parker, W., "Calculations of the Heat Release Rate by Oxygen Consumption for Various Applications," NBSIR 81-2427, National Bureau of Standards, Gaithersburg, MD, March 1982.
- [15] Siegel, R. and Howell, J.R., Thermal Radiation Heat Transfer, 2nd edition, McGraw-Hill Book Company, New York, NY, pg. 1, 1981.
- [16] Babrauskas, V., "Specimen Heat Fluxes for Bench-Scale Heat Release Rate Testing," Fire and Materials, Interflam '93, Fire Safety, International Interflam Conference, 6th, March 30-April 1, 1993, Oxford, England, Interscience Communications Ltd., London, England, pp. 57-74, 1993.
- [17] Madrzykowski, D., "Office Work Station Heat Release Rate Study: Full Scale vs. Bench Scale," Interflam '96, International Interflam Conference, 7th Proceedings, March 26-28, 1996, Cambridge, England, Interscience Communications, Ltd., London, England, pp. 47-55, 1996.
- [18] Taylor, B.N. and Kuyatt, C.E., "Guidelines for Evaluating and Expressing the Uncertainty of NIST Measurement Results," NIST TN 1297, National Institute of Standards and Technology, Gaithersburg, MD, January 1994.

- [19] Twilley, W. H. and Babrauskas, V., "User's Guide for the Cone Calorimeter," NBS SP 745, National Institute of Standards and Technology, Gaithersburg, MD, August 1988.
- [20] Bryant, R.A., Womeldorf, C.A., Johnsson, E.L., and Ohlemiller, T.J., "Radiative Heat Flux Measurement Uncertainty," Fire and Materials, Vol. 27, No. 5, pp. 209-222, 2003.



Figure 1. Photograph showing the front and one side of test structure with tile roof prior to start of test.



Figure 2. Photograph showing rear and one side of test structure with asphalt single roof prior to start of test.

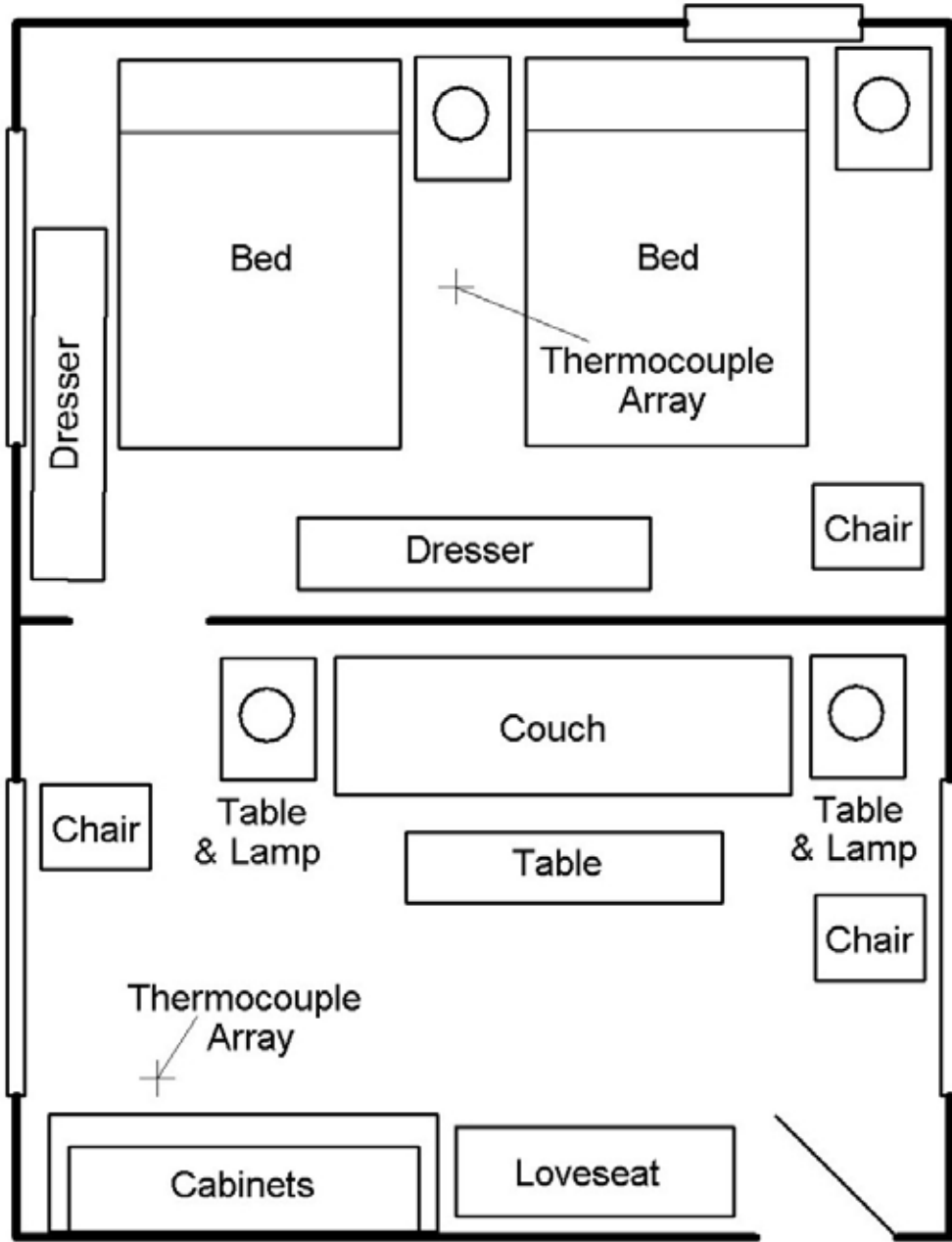


Figure 3. Plan view of generic test structure showing approximate placement of furniture and other items within structure (not to scale).

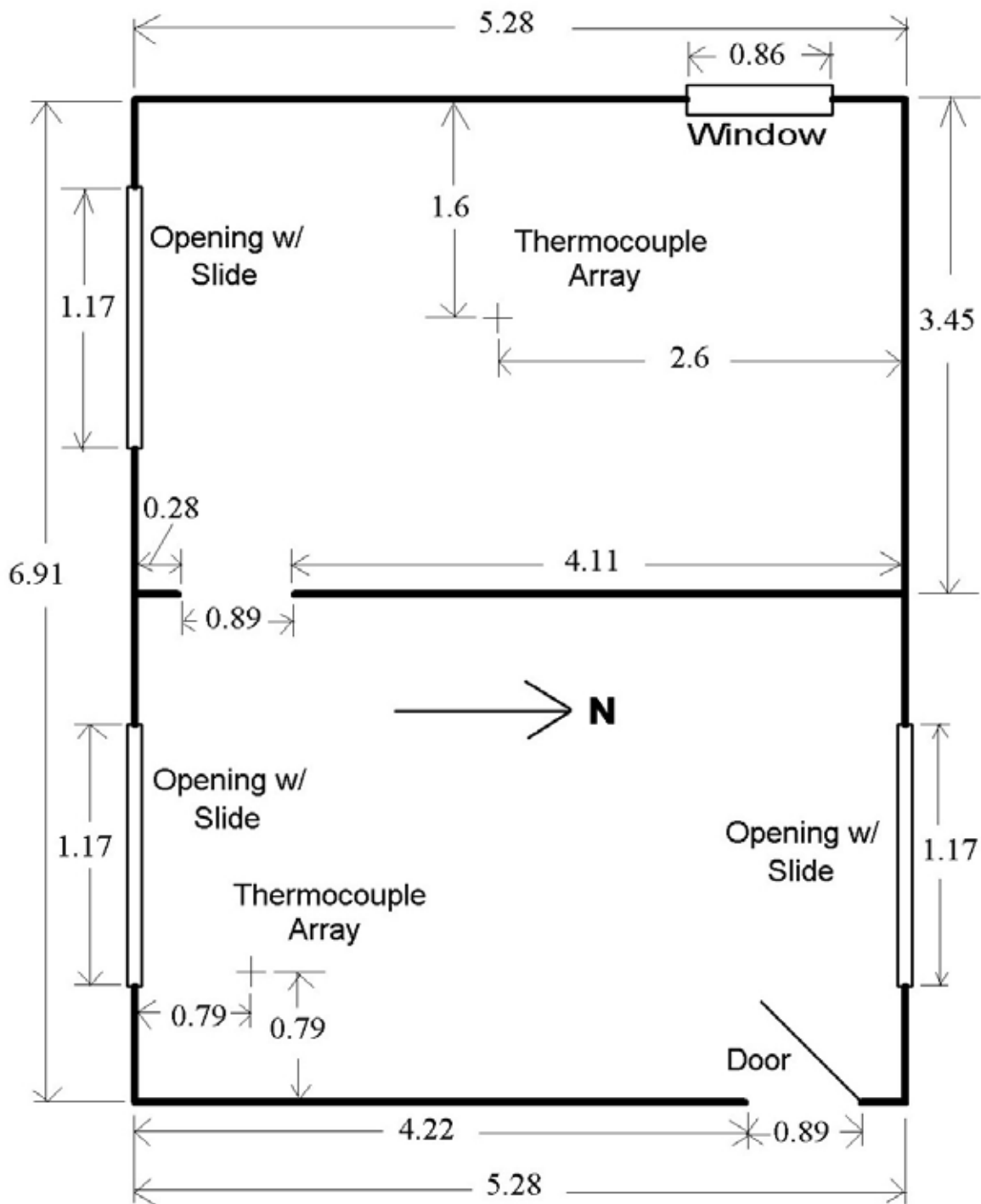


Figure 4. Plan view of generic structure showing locations of measurement instruments and dimensions (all dimensions in m).

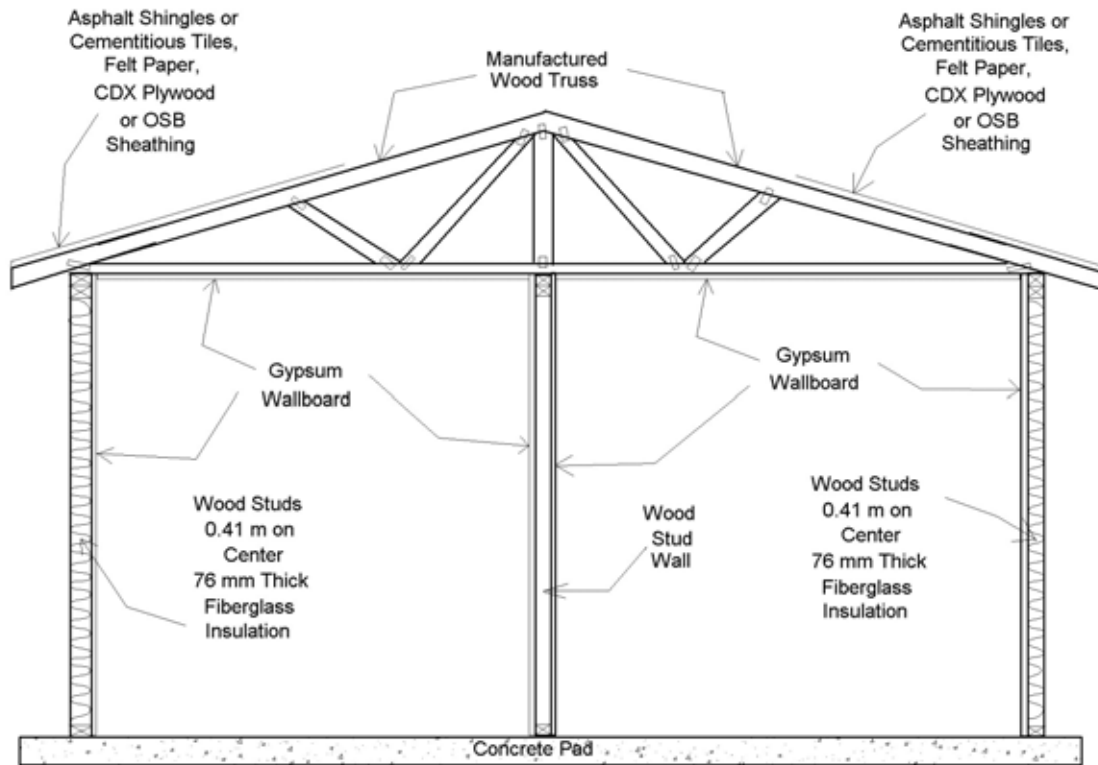


Figure 5. Diagram showing typical construction of the structure.



Figure 6. Photograph showing “living room” ceiling with ceiling louvers, electrical boxes, and attic access.



Figure 7. Photograph of “living room” area showing furniture arrangement.



Figure 8. Photograph showing “living room” with furniture, cabinets, and thermocouple array.



Figure 9. Photograph showing furniture in “bedroom” area of test structure. (A thermocouple array is visible in the foreground.)



Figure 10. Photograph showing two double beds, night tables and lamps in the “bedroom”.



Figure 11. Photograph showing trusses supporting the roof structure with thermocouple array visible in front of second vertical wood member.



Figure 12. Photograph of “living room” showing ignition location in corner of couch under newspaper.



Figure 13. Photograph showing “bedroom” with ignition location in corner of chair under the newspaper.



Figure 14. Photograph of test structure at 60 s after ignition.



Figure 15. Photograph of test structure at 75 s after ignition.



Figure 16. Photograph of test structure at 120 s after ignition.



Figure 17. Photograph of test structure at 180 s after ignition.



Figure 18. Photograph of test structure at 210 s after ignition.



Figure 19. Photograph of test structure at 540 s after ignition.



Figure 20. Photograph of test structure at 640 s after ignition.



Figure 21. Photograph of test structure at 900 s after ignition when front door has burned away.



Figure 22. Photograph of test structure at 960 s after ignition with portion of roof structure burning.



Figure 23. Photograph of test structure at 1010 s after ignition as collapse is starting.



Figure 24. Photograph of test structure at 1140 s after ignition when suppression has been completed.

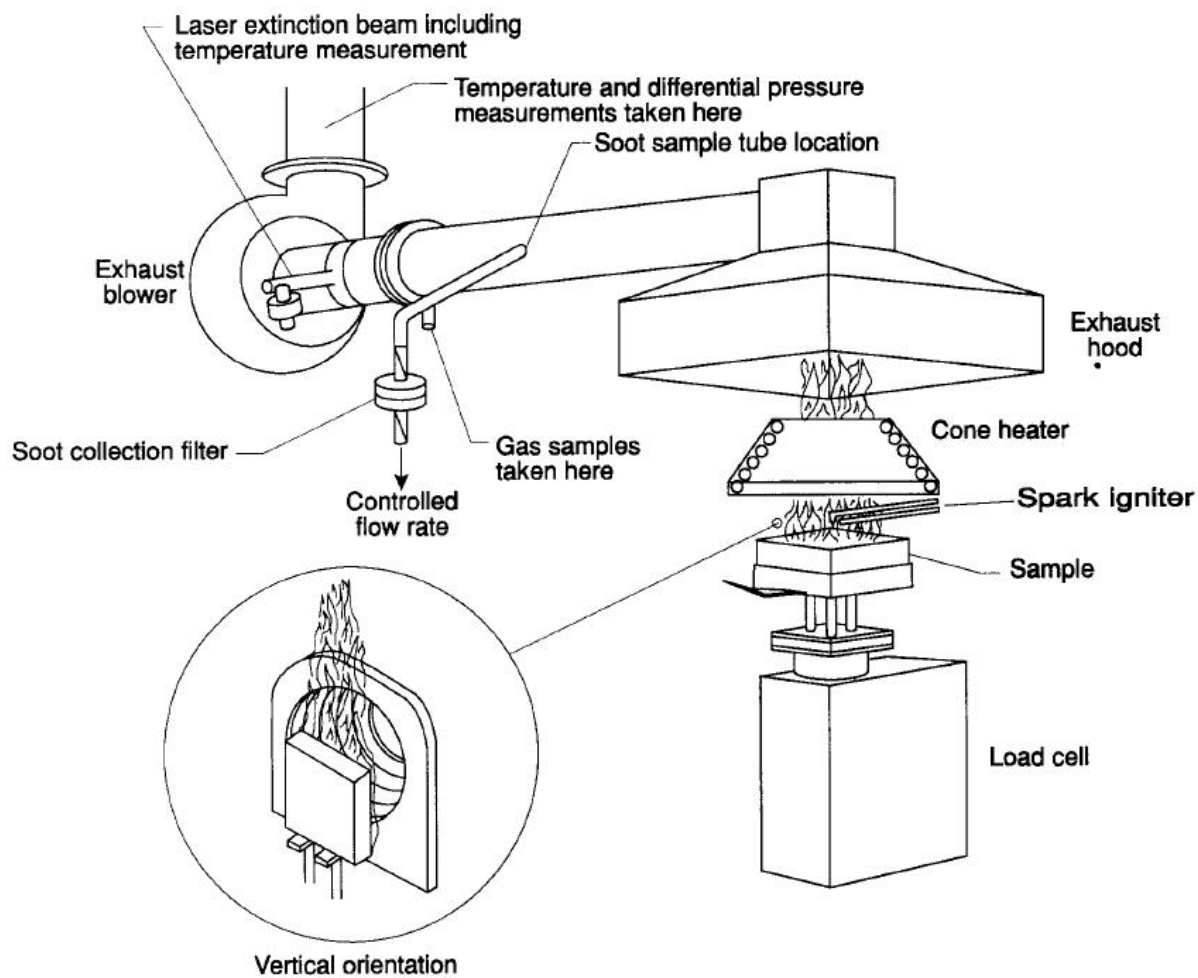


Figure 25. Schematic drawing of the cone calorimeter.

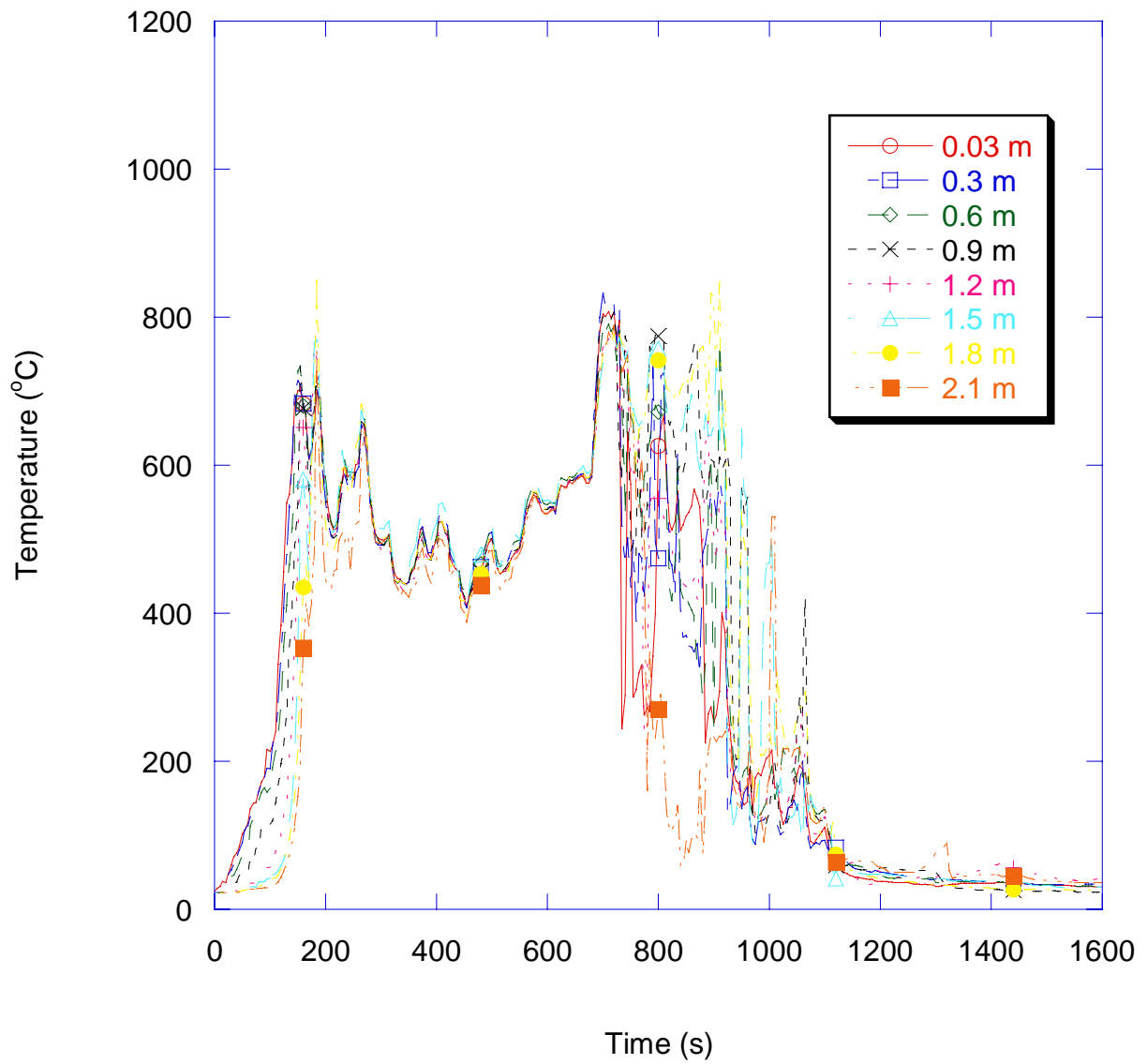


Figure 26. Graph showing temperatures measured in the living room during the first test (distances measured from ceiling downward).

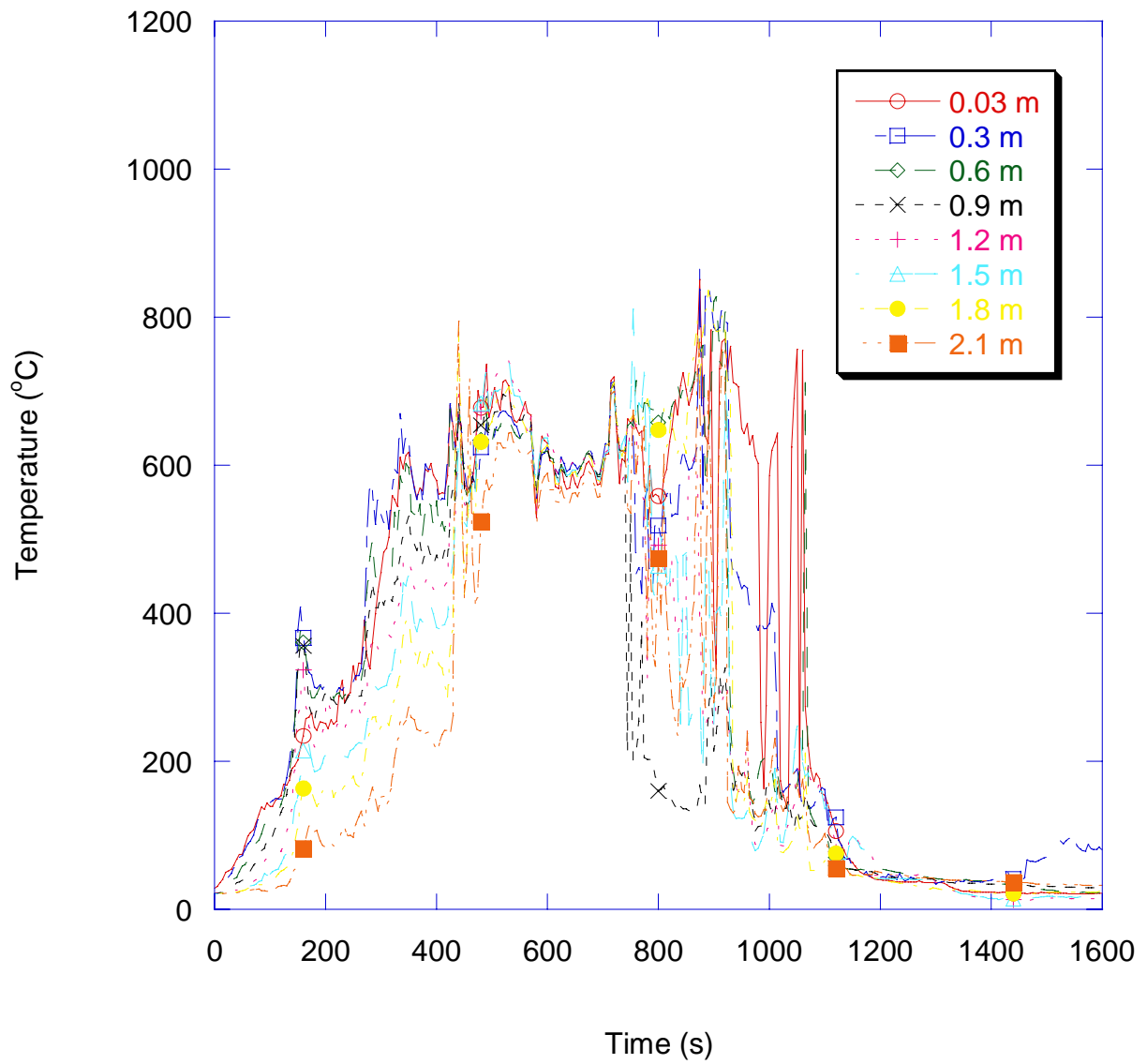


Figure 27. Graph showing temperatures measured in the bedroom during the first test (distances measured from ceiling downward).

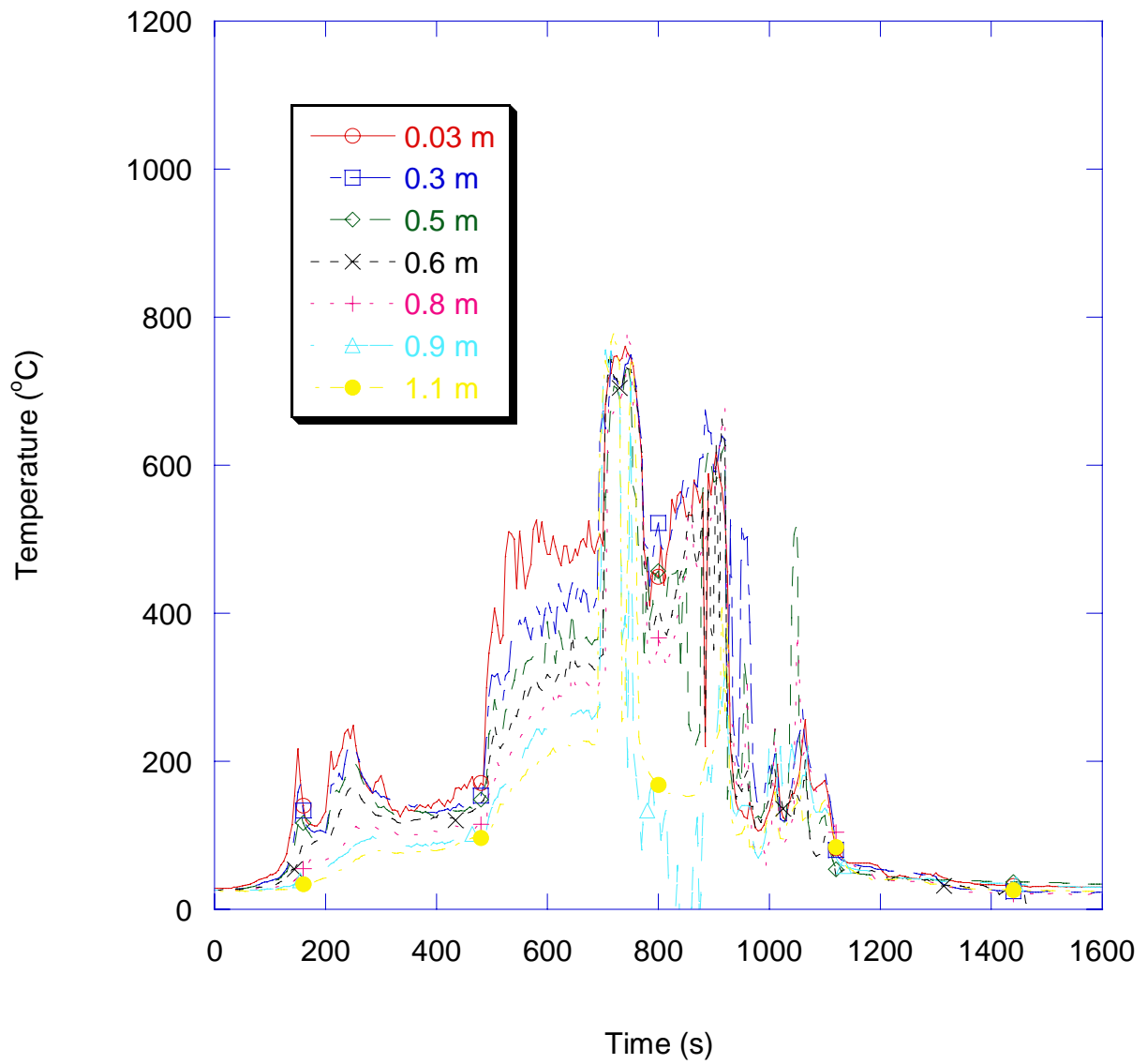


Figure 28. Graph showing temperatures measured in the north portion of the attic during the first test (distances measured from roof peak downward).

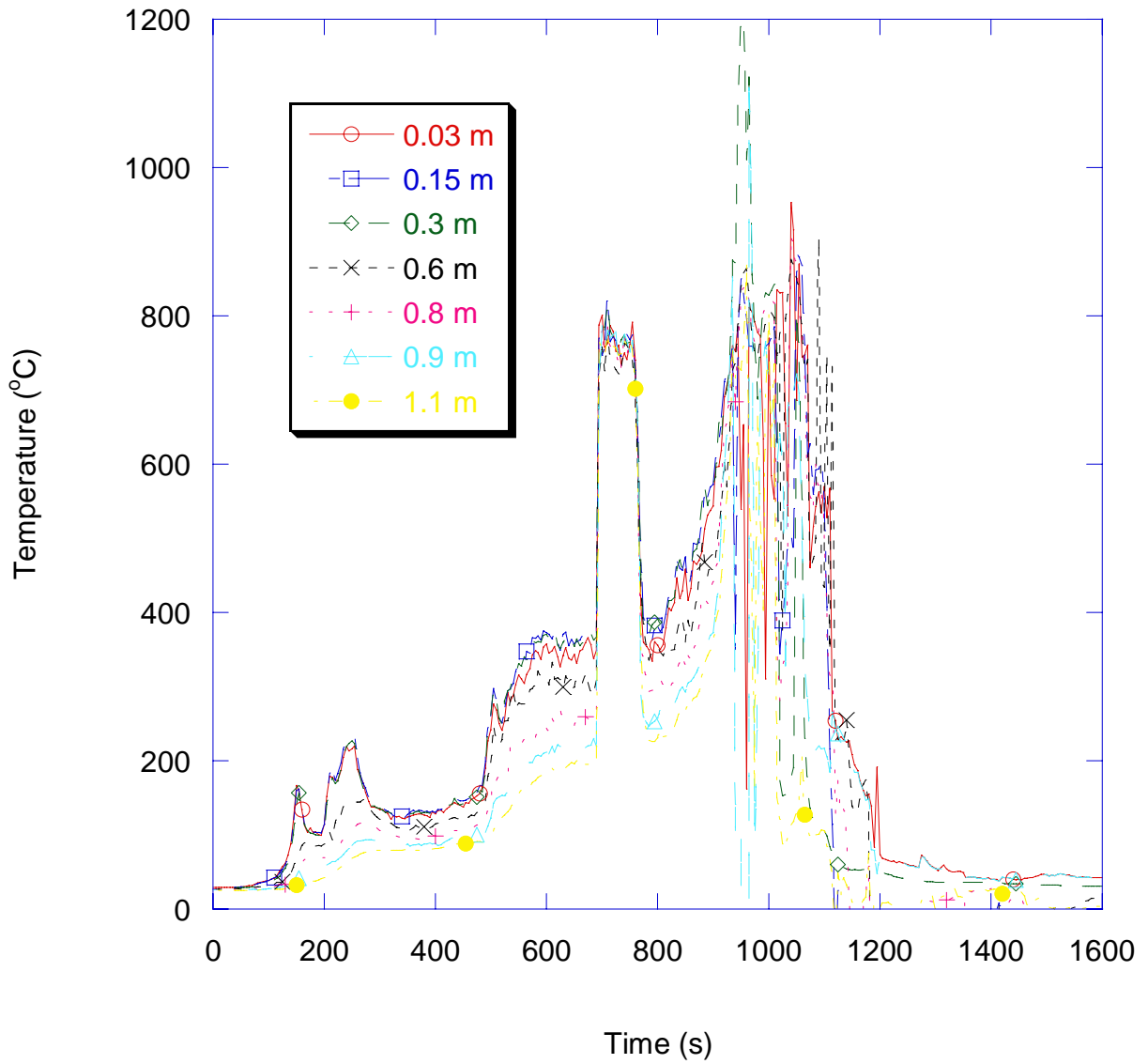


Figure 29. Graph showing temperatures measured in the south portion of the attic during the first test (distances measured from roof peak downward).

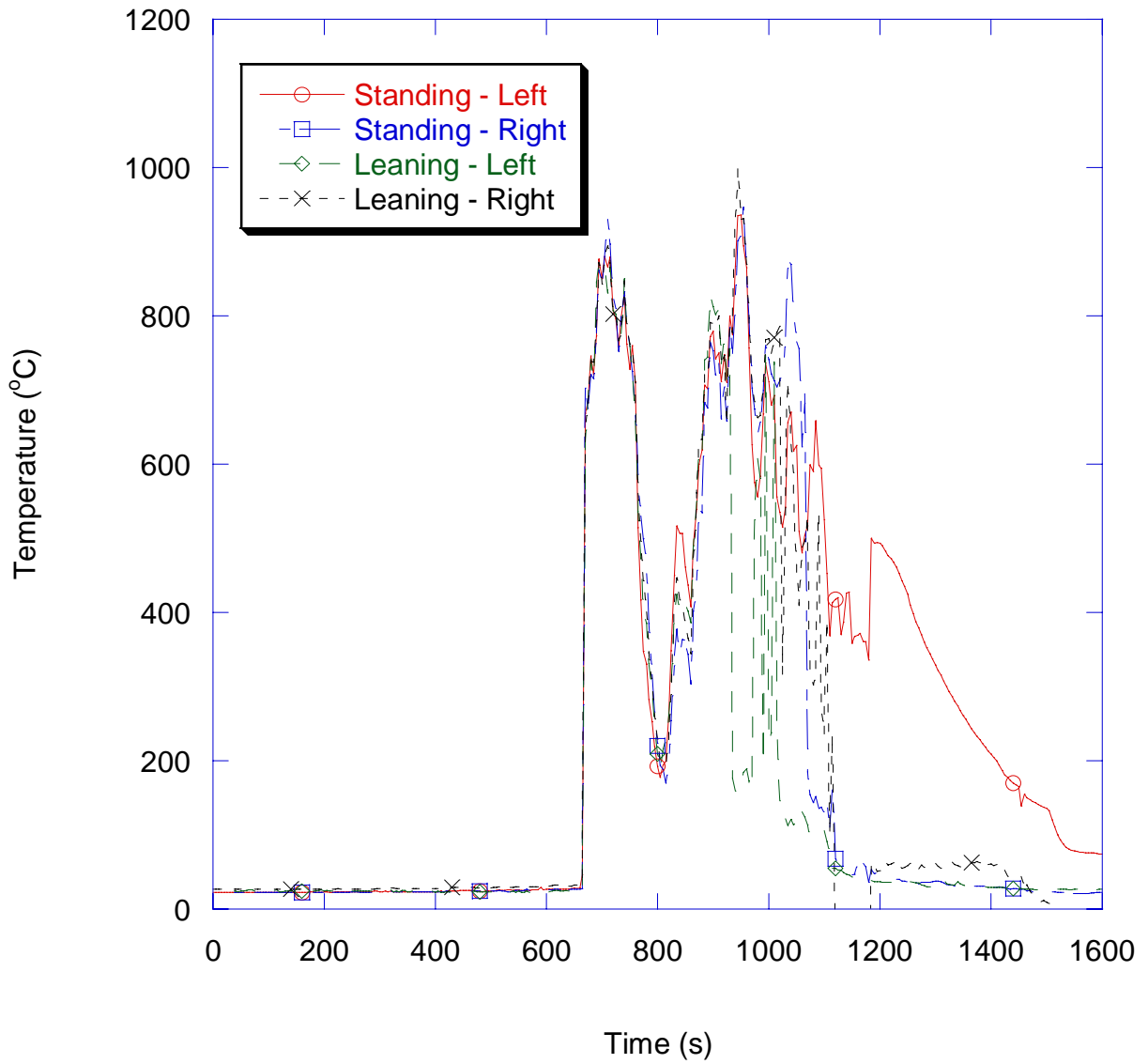


Figure 30. Graph showing temperatures measured on the roof under the fire fighter mannequins' boots during the first test.

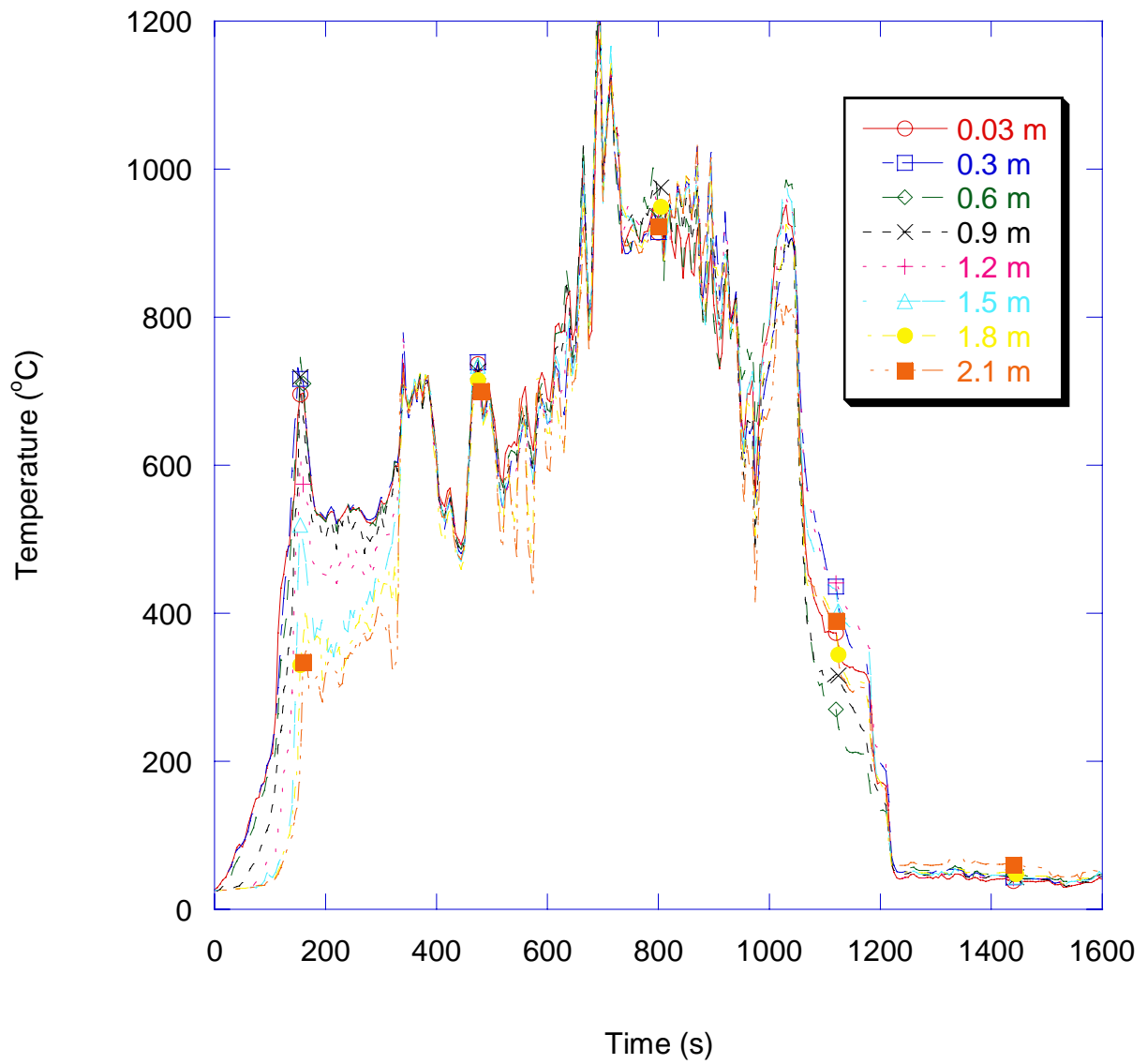


Figure 31. Graph showing temperatures measured in the living room during the second test (distances measured from ceiling downward).

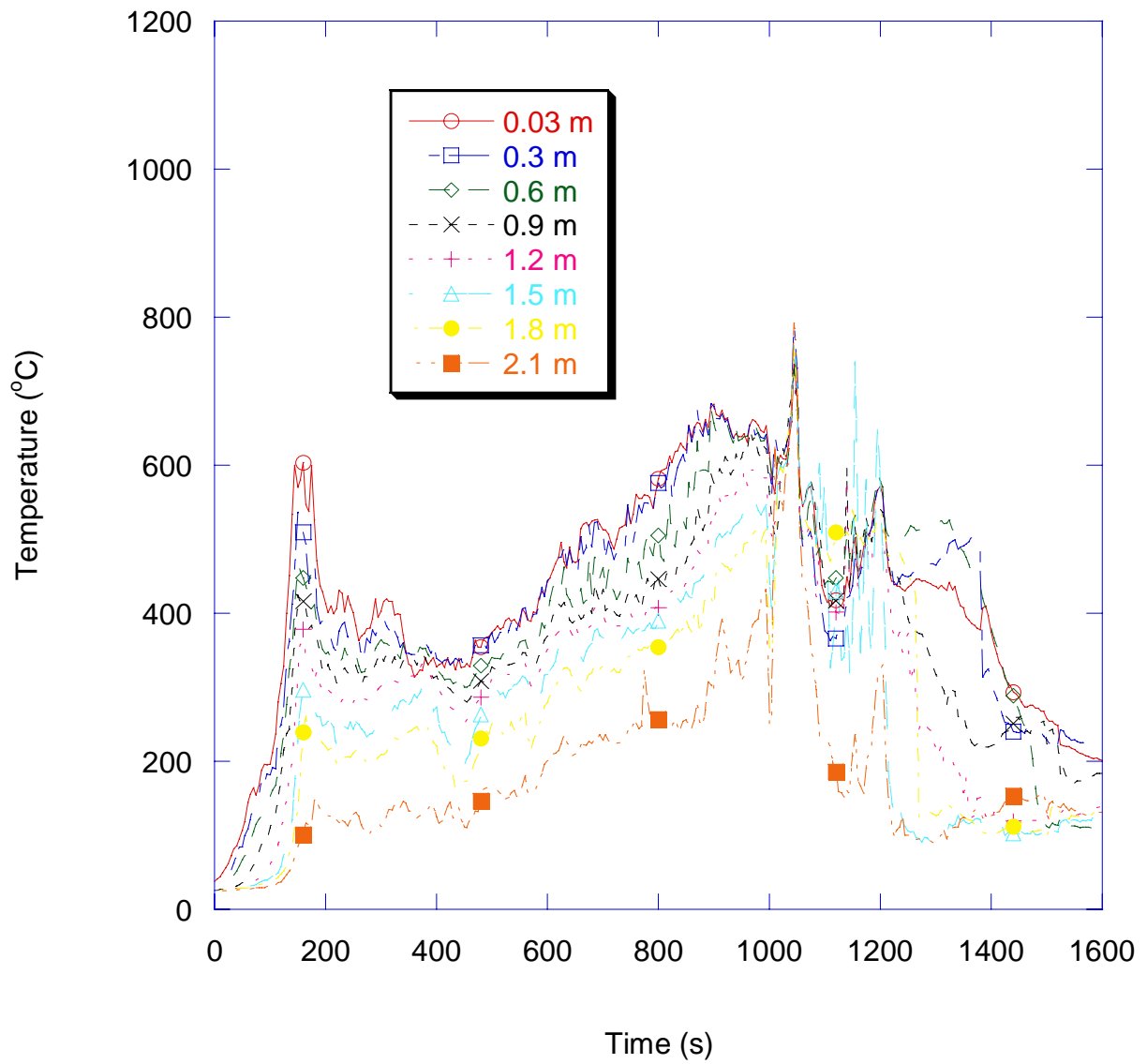


Figure 32. Graph showing temperatures measured in the bedroom during the second test (distances measured from ceiling downward).

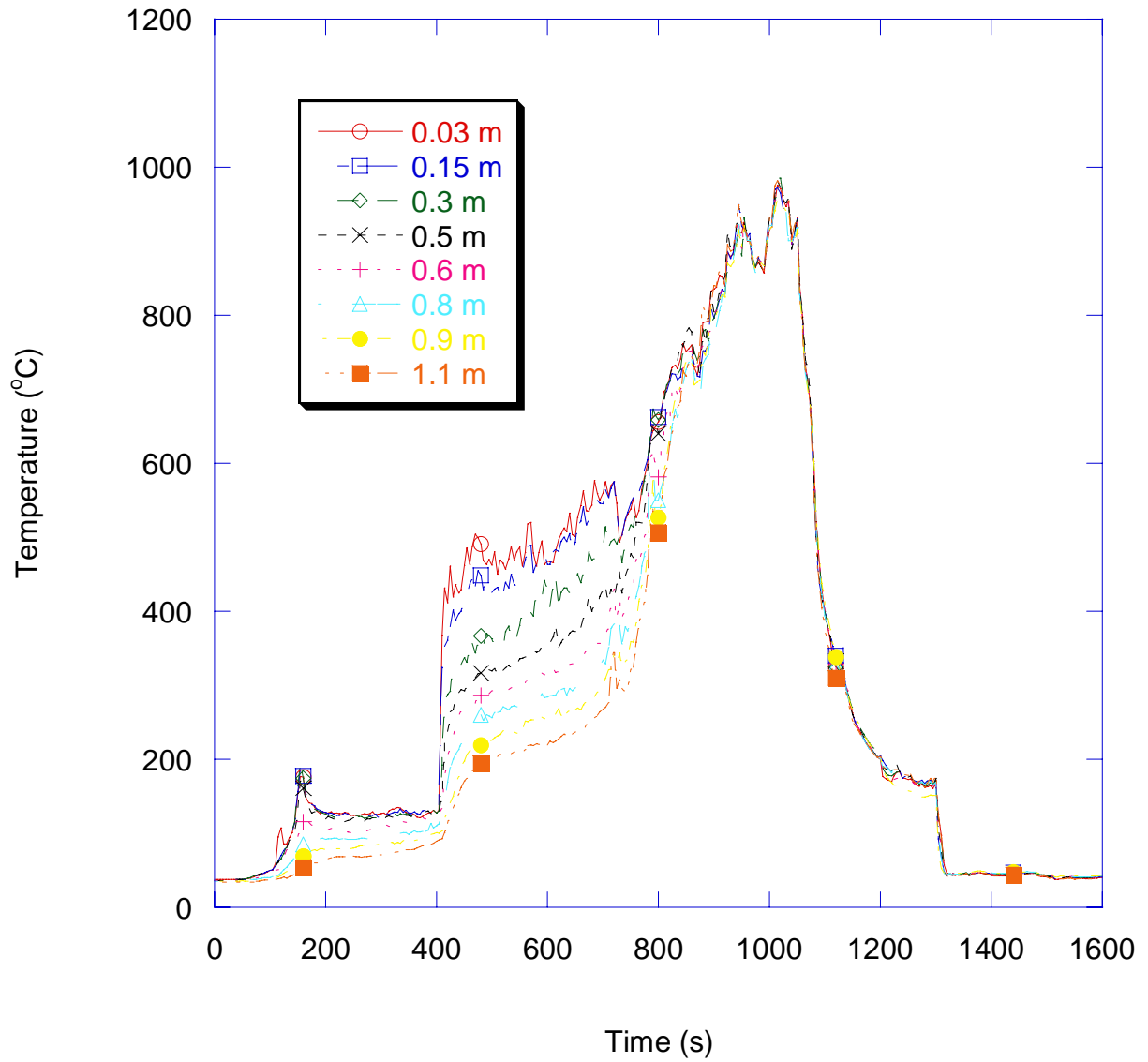


Figure 33. Graph showing temperatures measured in the north portion of the attic during the second test (distances measured from roof peak downward).

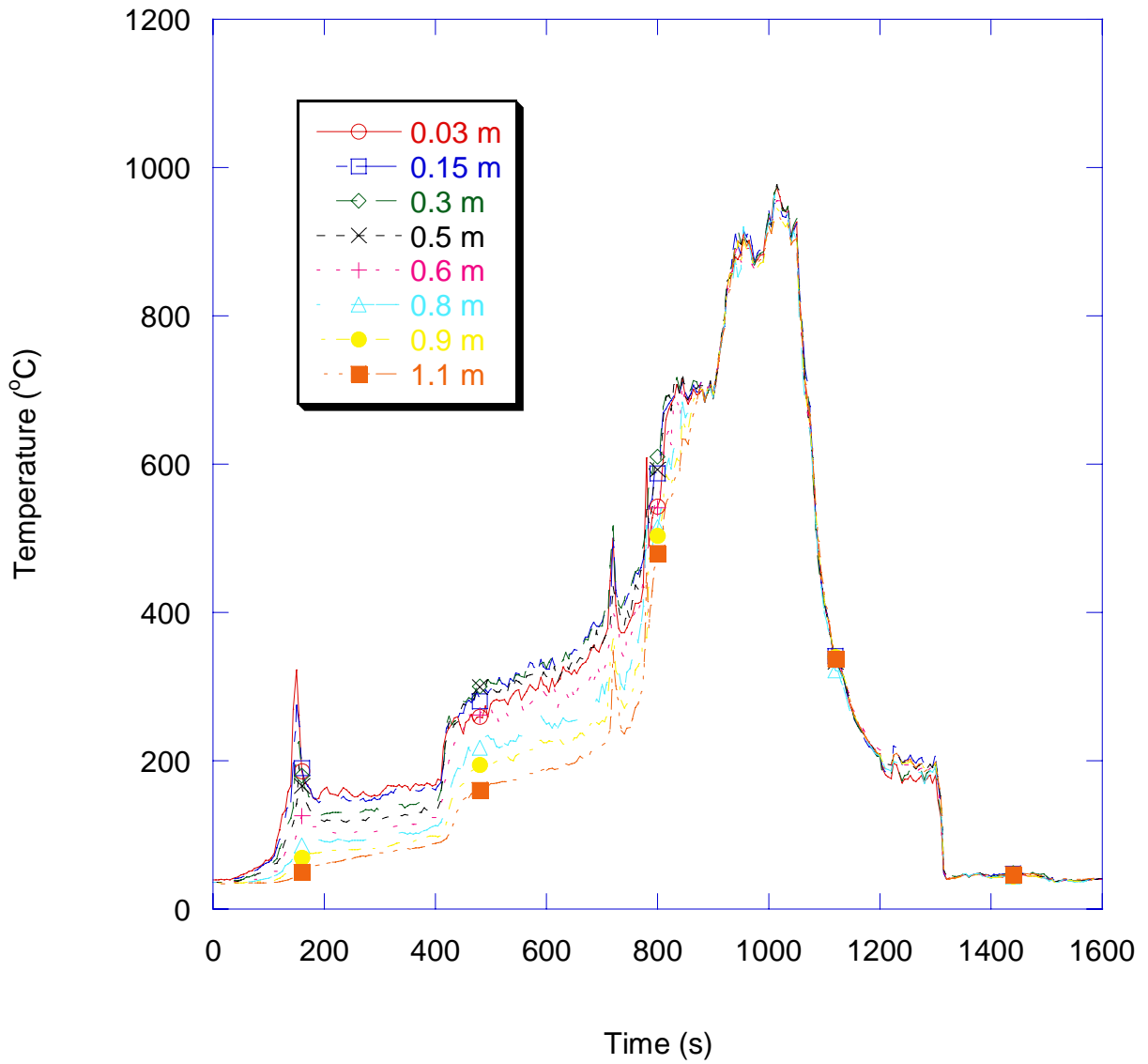


Figure 34. Graph showing temperatures measured in the south portion of the attic during the second test (distances measured from roof peak downward).

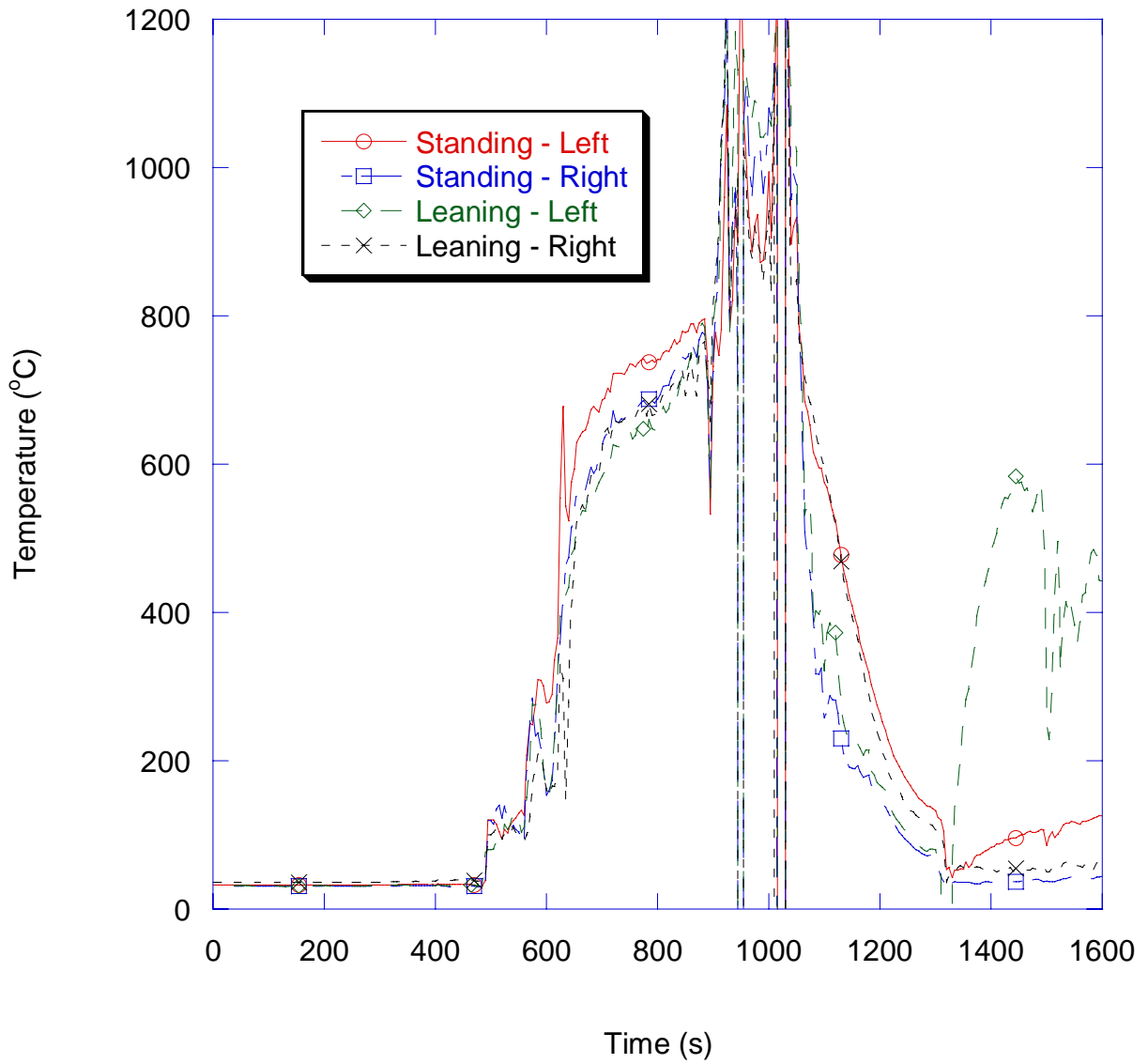


Figure 35. Graph showing temperatures measured on the roof under the fire fighter mannequins' boots during the second test.

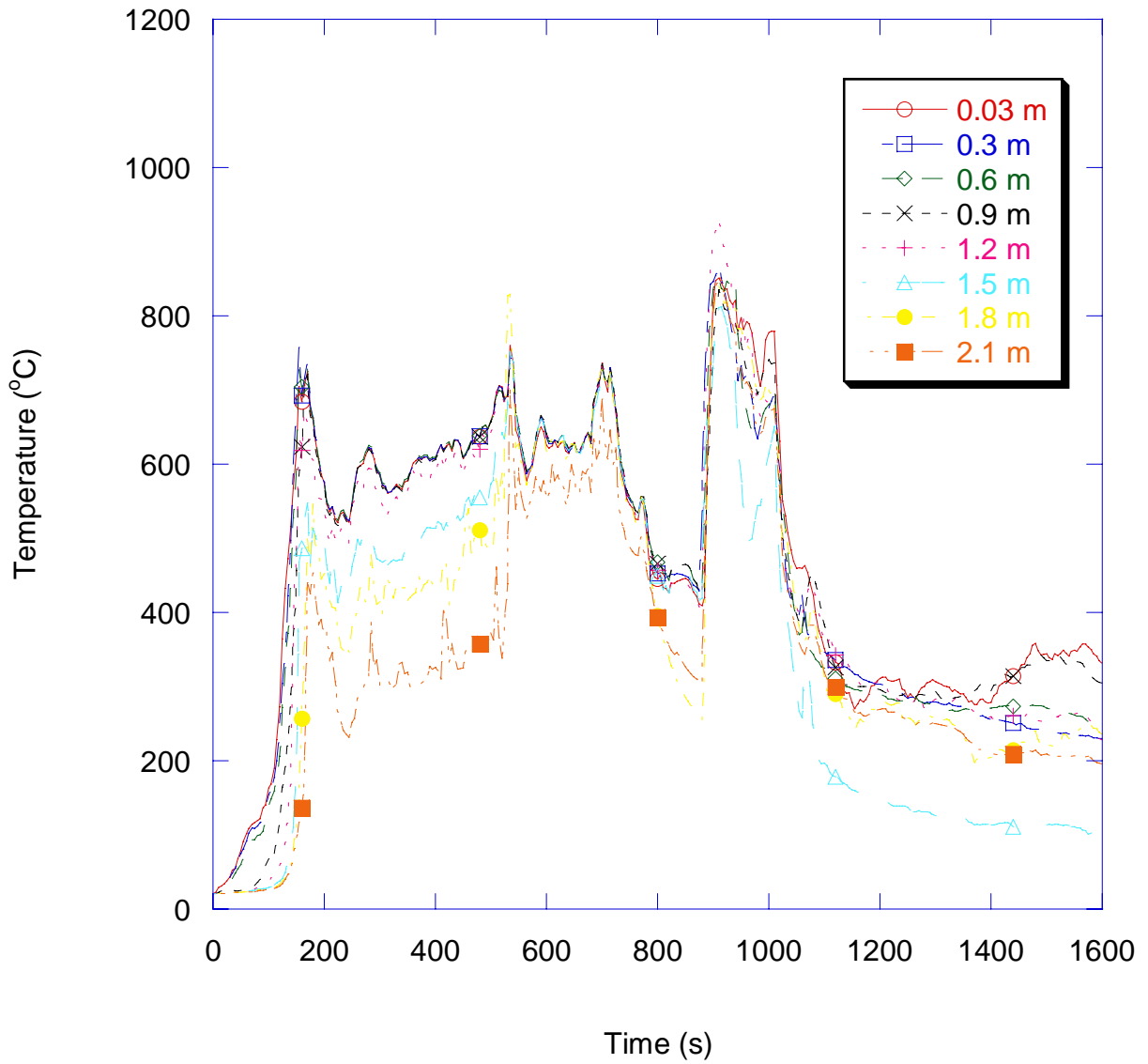


Figure 36. Graph showing temperatures measured in the living room during the third test (distances measured from ceiling downward).

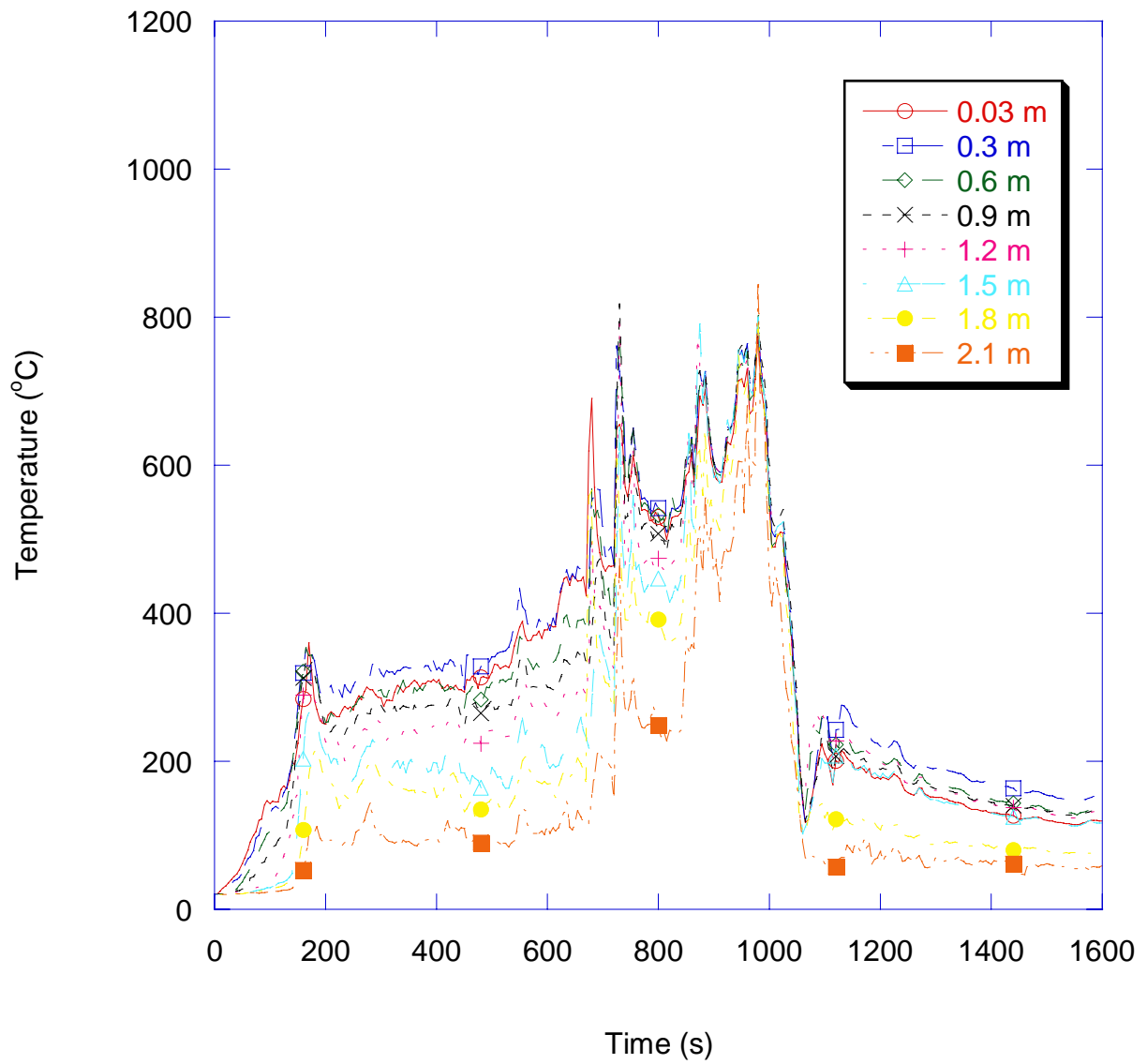


Figure 37. Graph showing temperatures measured in the bedroom during the third test (distances measured from ceiling downward).

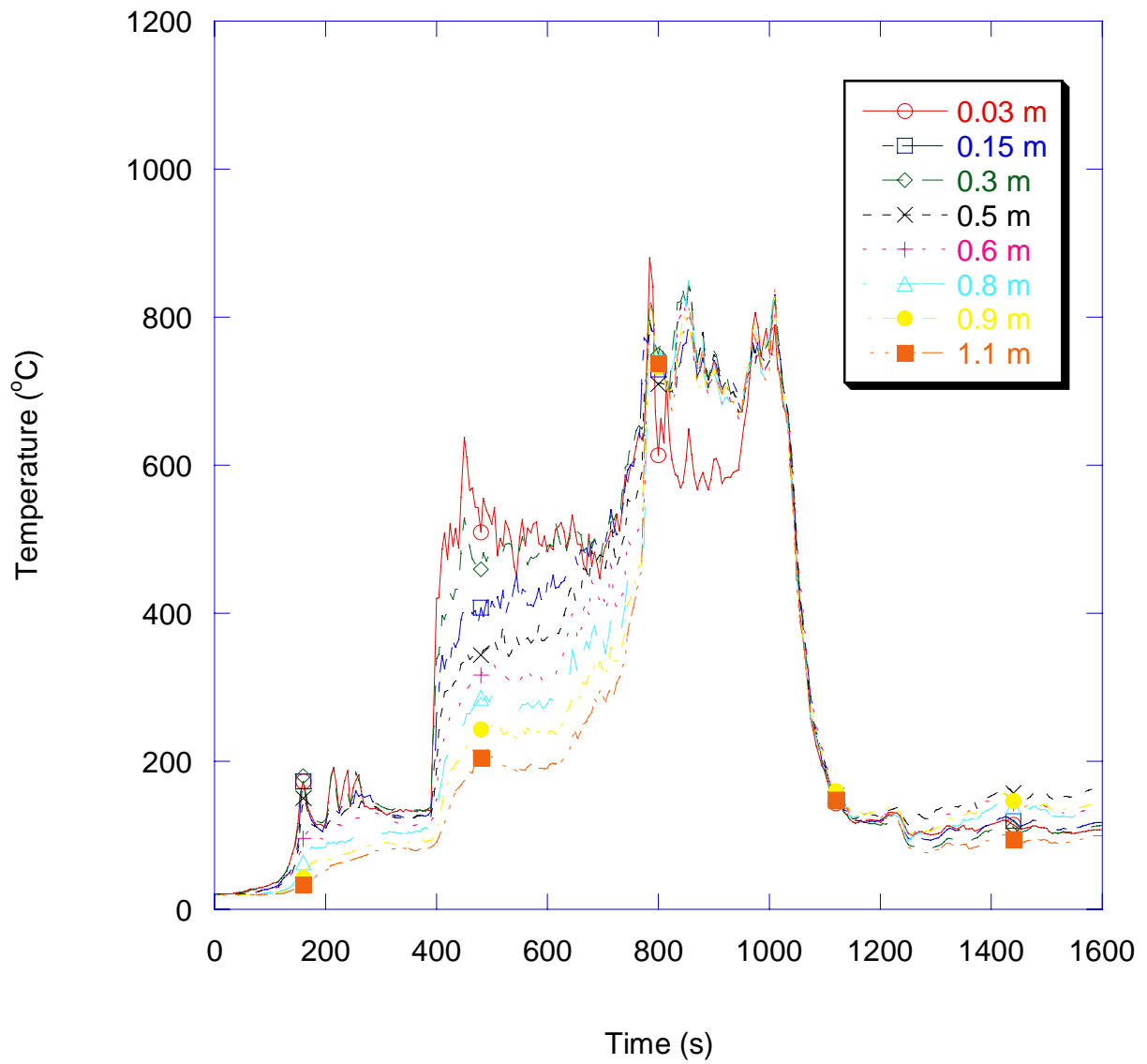


Figure 38. Graph showing temperatures measured in the north portion of the attic during the third test (distances measured from roof peak downward).

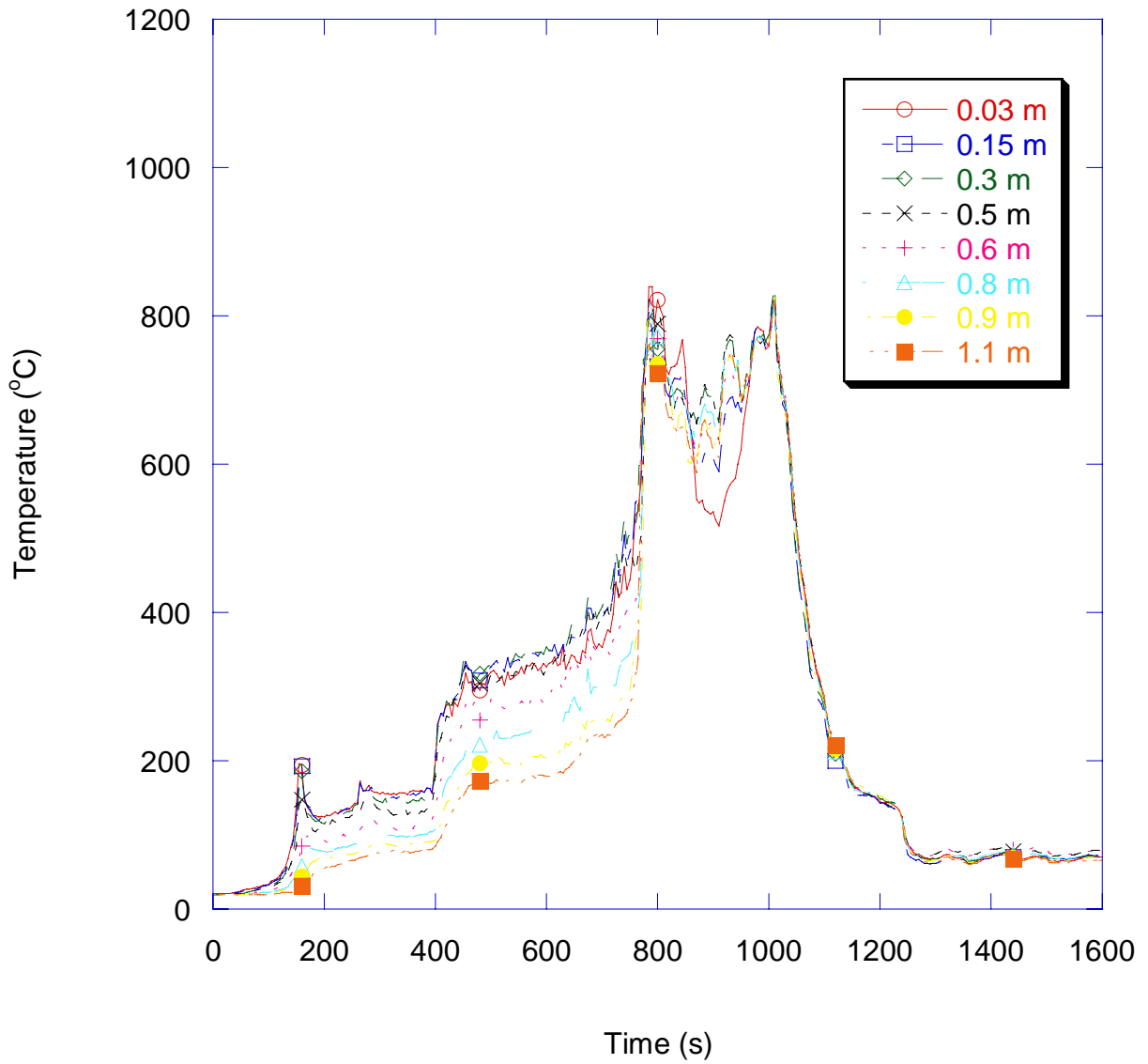


Figure 39. Graph showing temperatures measured in the south portion of the attic during the third test (distances measured from roof peak downward).

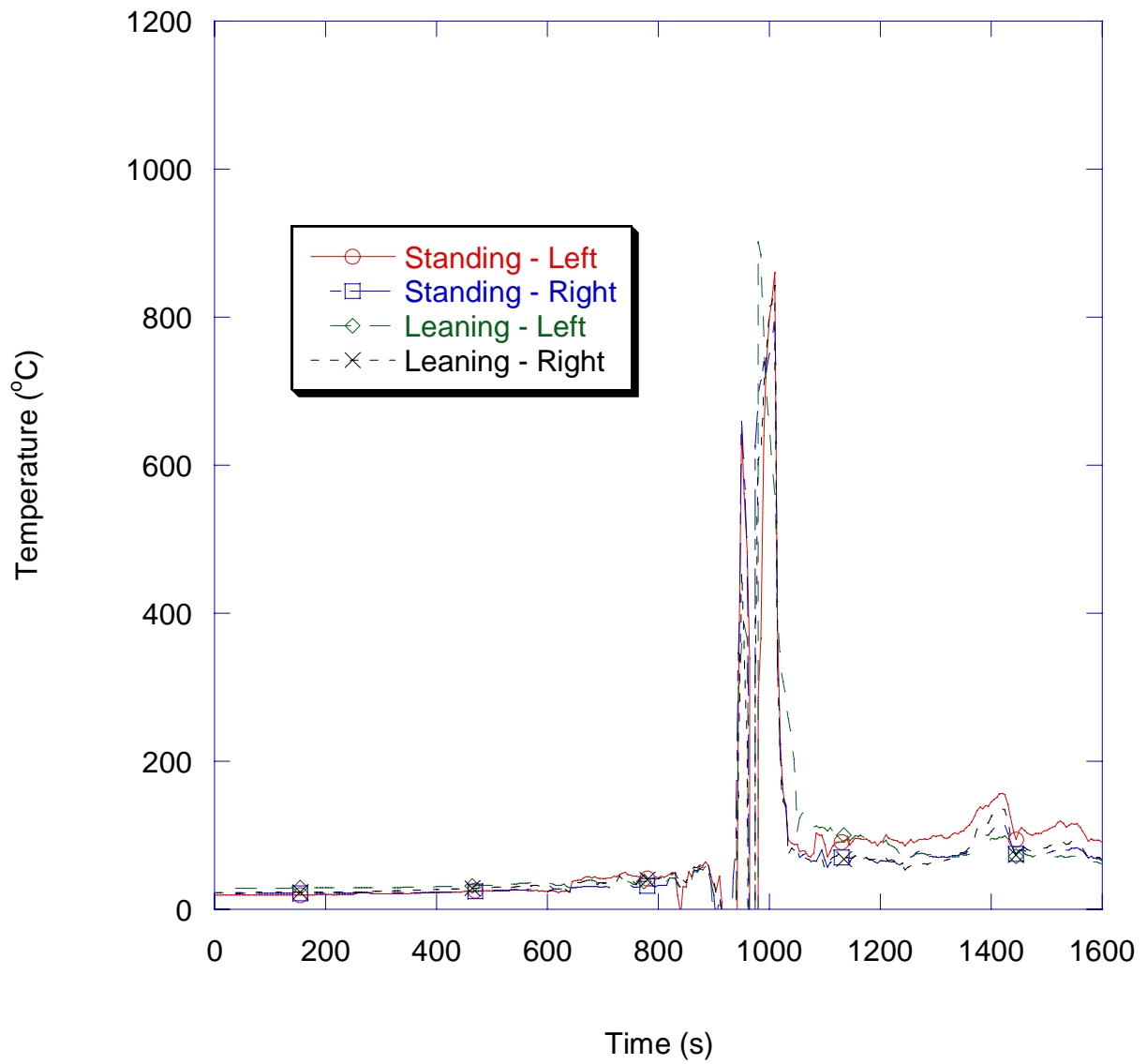


Figure 40. Graph showing temperatures measured on the roof under the fire fighter mannequins' boots during the third test.

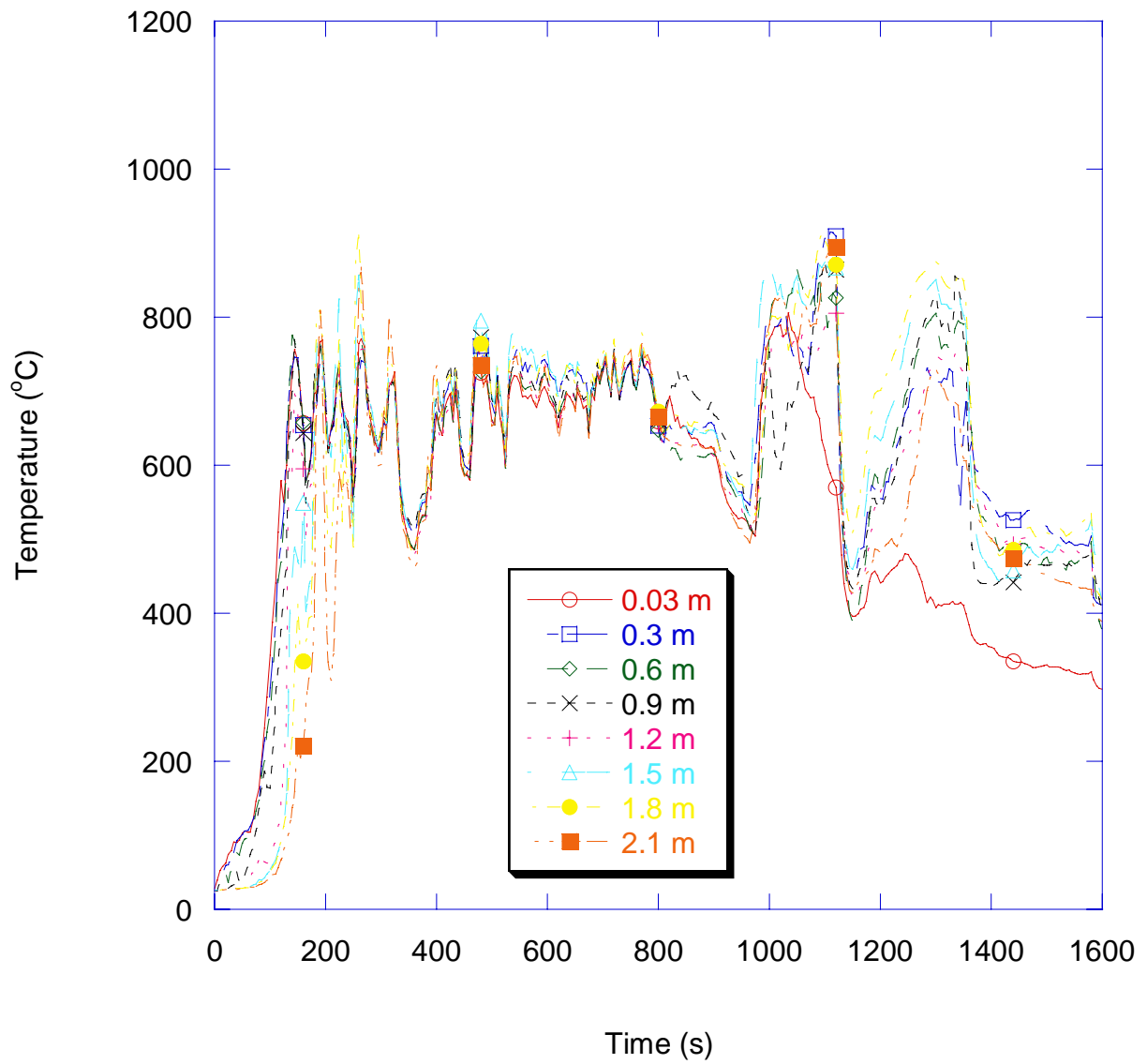


Figure 41. Graph showing temperatures measured in the living room during the fourth test (distances measured from ceiling downward).

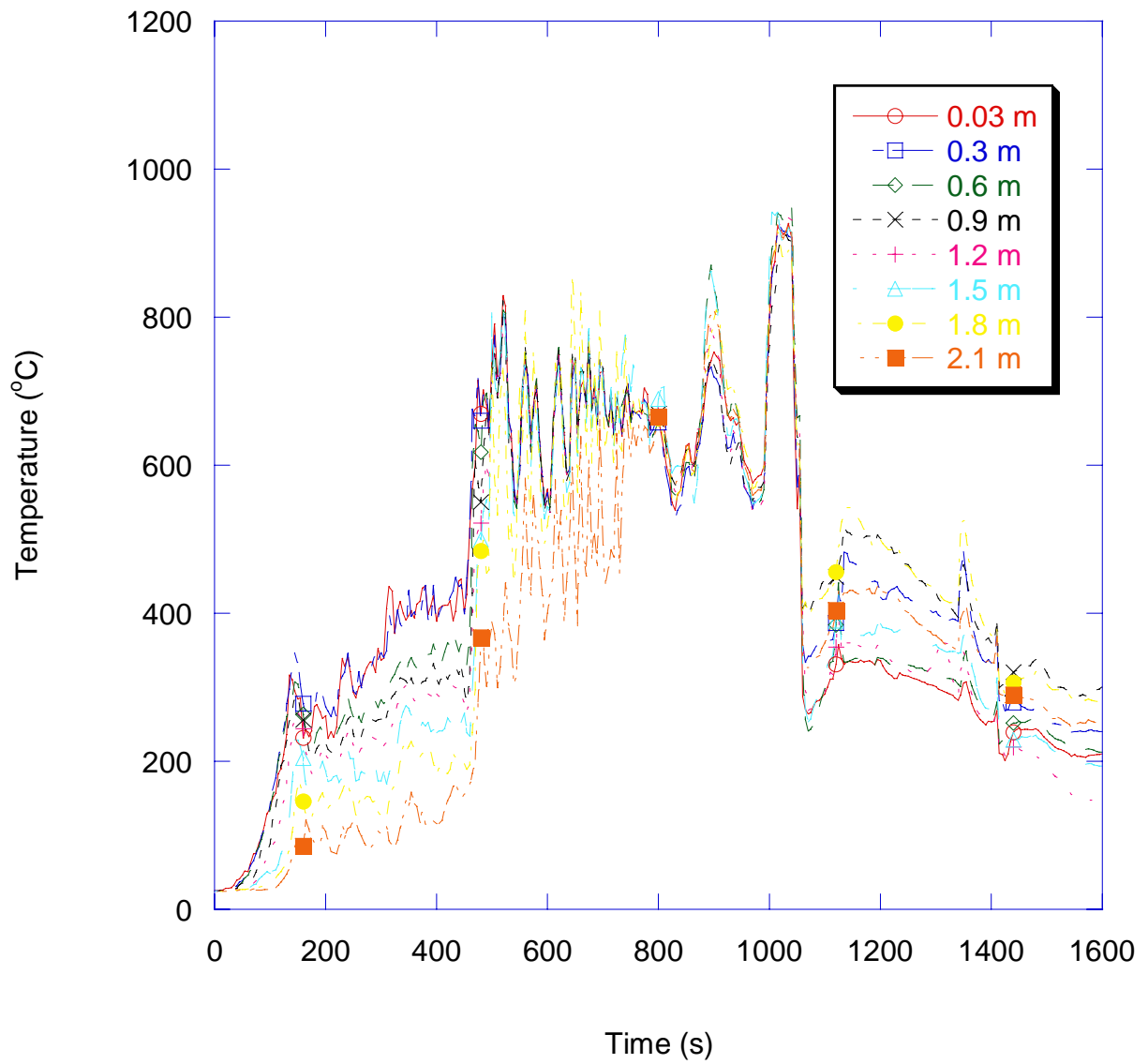


Figure 42. Graph showing temperatures measured in the bedroom during the fourth test (distances measured from ceiling downward).

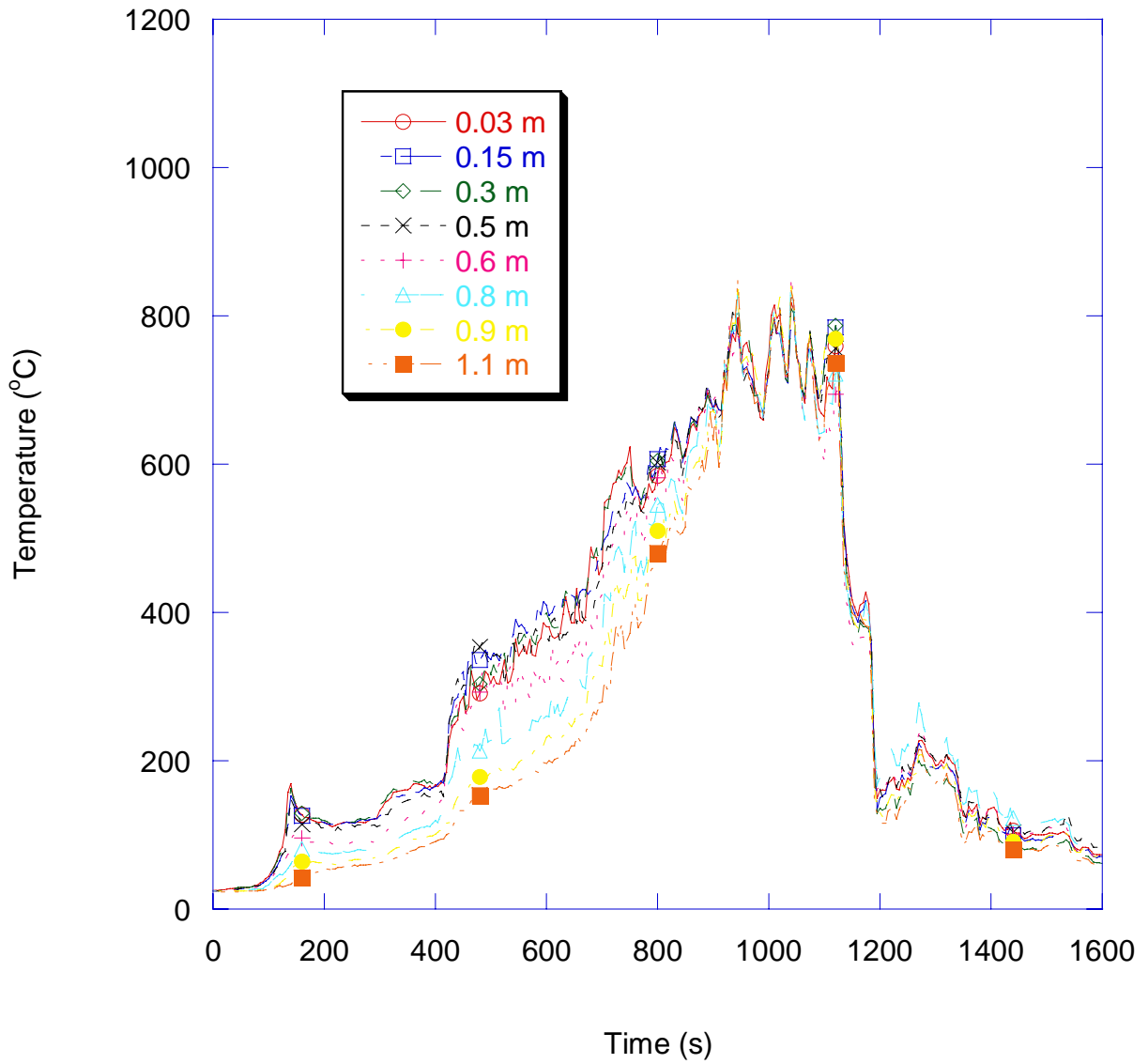


Figure 43. Graph showing temperatures measured in the north portion of the attic during the fourth test (distances measured from roof peak downward).

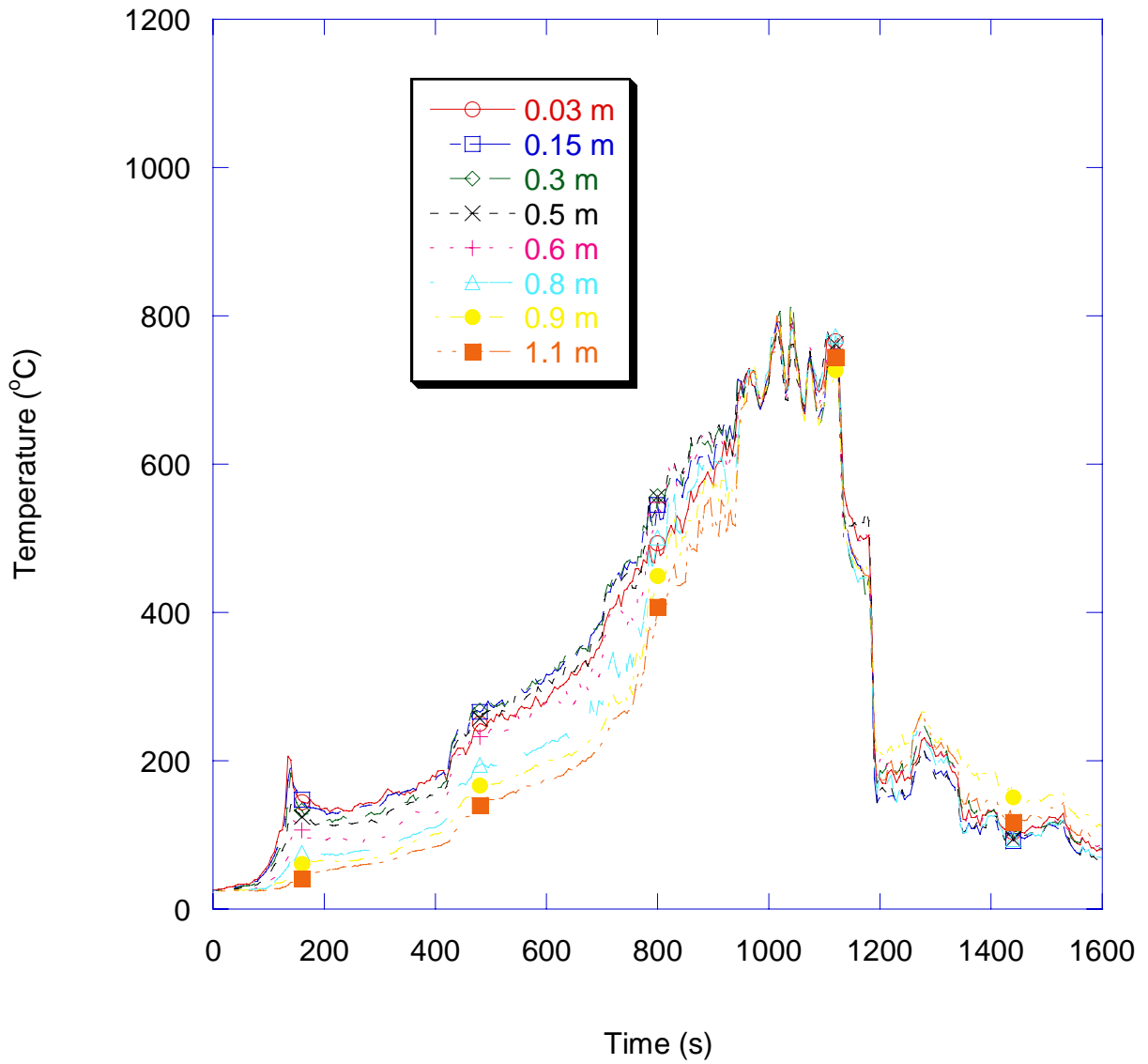


Figure 44. Graph showing temperatures measured in the south portion of the attic during the fourth test (distances measured from roof peak downward).

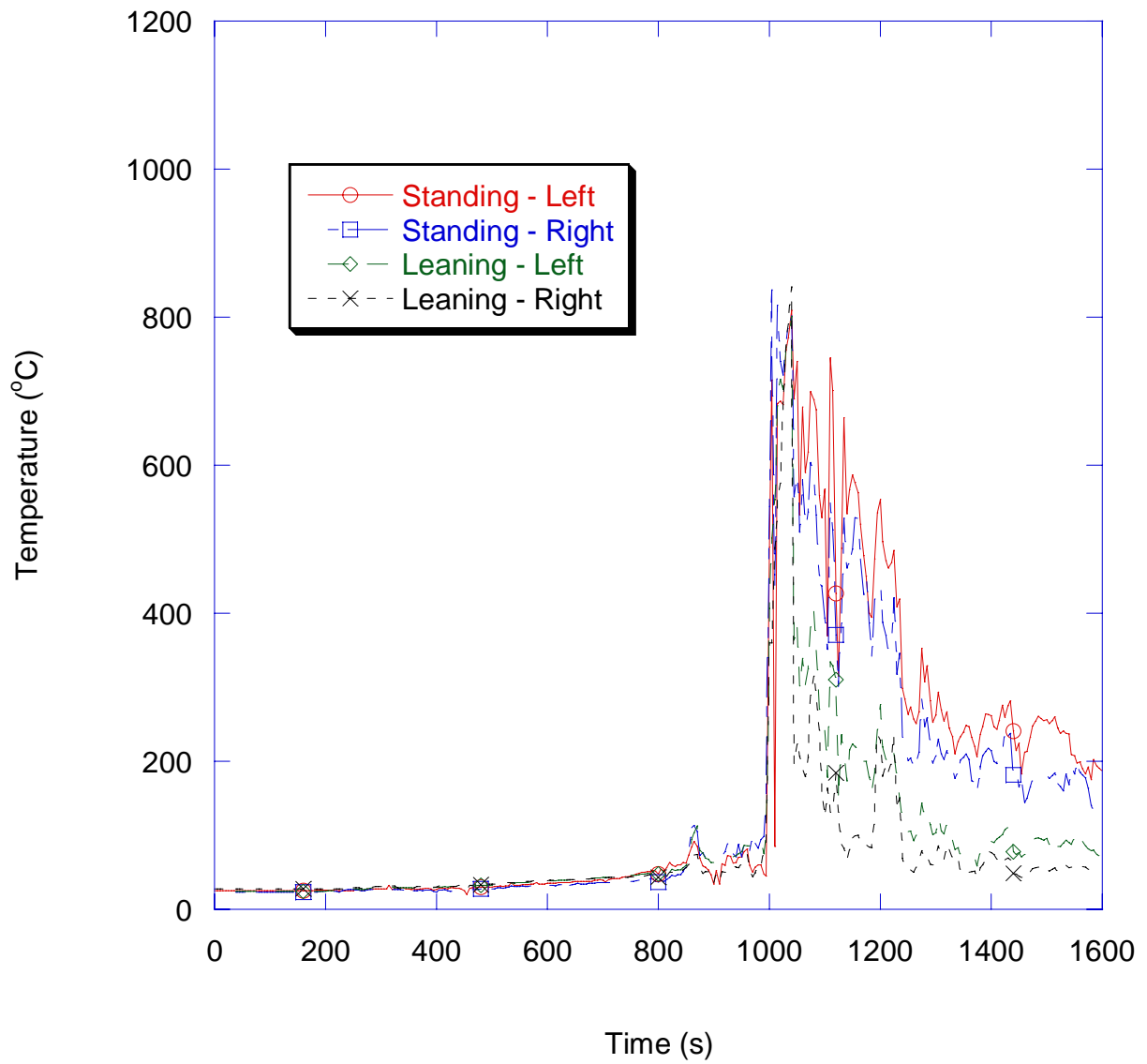


Figure 45. Graph showing temperatures measured on the roof under the fire fighter mannequins' boots during the fourth test.

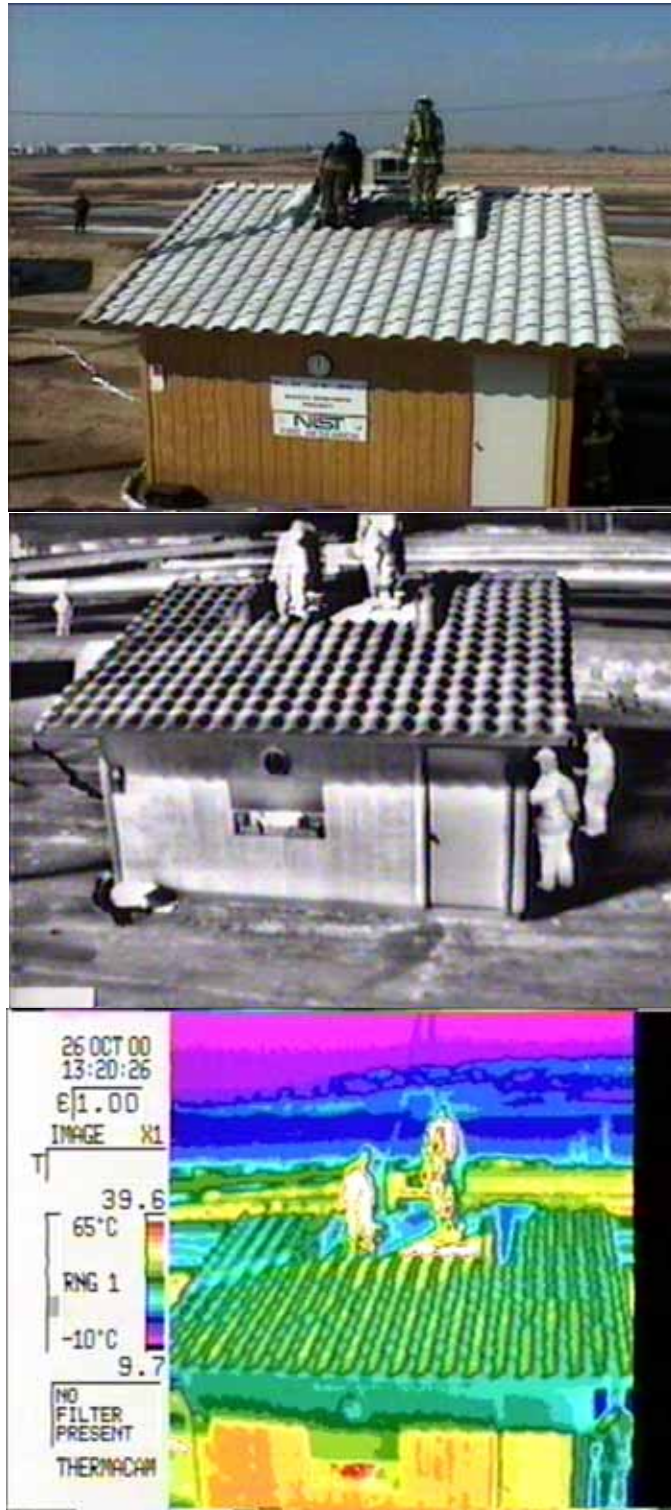


Figure 46. Test 3 shown a few seconds after ignition (top – normal video, middle – fire department thermal imager, bottom – high end, quantitative infrared camera)



Figure 47. Test 3 shown approximately 10 s before collapse of the roof structure (top – normal video, middle – fire department thermal imager, bottom – high end, quantitative infrared camera)

Appendix A
Cone Calorimeter Test Data

FILE: C:\CONE171\RAWDATA\010731A1.CDT

----- Test Parameters -----

Test Date : 31-Jul-01 Test Time : 13:38 p.m. Operator : Michael Smith

Test Scans : 238 scans, 3 secs/scan
 Test Length : 592.94 secs
 Sample Surface Area : 0.01000 m2
 Radiant Heat Flux : 35.0 kW/m2
 Sample Orientation : Horizontal
 Measured Exh. Flow : 0.024 m3/sec
 Orifice Plate : 57 mm
 Sample Material :
 External Oriented Strandboard
 SAMP.1

----- Test Notes -----

Pre-test Comments:
 Samp.in double density alumn.pan edge control.
 Thermal absorber applied.
 Samp.wt.=77.4g,Samp.+pan wt.=80.5g.
 All samp.this series are 100mm X 100mm X 12mm

Post-test Comments:
 Samp.exhibited a uniform combustion process
 without any thermal anomalies to report.

----- Reduction Parameters -----

C-Factor (Methane) : 0.04381603
 Conversion Factor : 13.100 MJ/kg 02
 Baseline O2 Reading : 20.984 %
 Baseline CO2 Reading : 0.04818%
 Baseline CO Reading : 0.00012 %

----- Test Results -----

Peak Heat Release Rate : 224.27 kW/m2 at 484.00 secs
 Average Heat Release Rate : 151.12 kW/m2
 Average Heat Release Rate T60 : 154.68 kW/m2
 Average Heat Release Rate T180: 154.38 kW/m2
 Average Heat Release Rate T300: 138.36 kW/m2
 Total Heat Released : 83.06 MJ/m2
 Average Effective HOC : 13.24 MJ/kg
 Average Specific Ext Area : 56.28 m2/kg
 Average Mass Loss Rate: : 11.783 g/s*m2
 Entered Initial Specimen Mass : 80.50 g
 Measured Final Specimen Mass : 17.75 g
 Average CO Yield : 0.00262 kg/kg
 Average CO2 Yield : 1.43264 kg/kg
 Time to sustained Ignition : 48.51 secs

FILE: C:\CONE171\RAWDATA\010731A2.CDT

----- Test Parameters -----

Test Date : 31-Jul-01 Test Time : 01:01 p.m. Operator : Michael Smith

Test Scans : 203 scans, 3 secs/scan
 Test Length : 487.16 secs
 Sample Surface Area : 0.01000 m2
 Radiant Heat Flux : 35.0 kW/m2
 Sample Orientation : Horizontal
 Measured Exh. Flow : 0.024 m3/sec
 Orifice Plate : 57 mm
 Sample Material :
 External Oriented Strandboard
 SAMP.2

----- Test Notes -----

Pre-test Comments:
 Samp.in double density alumn.pan edge control.
 Thermal absorber applied.
 Samp.wt.=68.2g,Samp.+pan wt.=71.4g.

Post-test Comments:
 Samp.exhibited a uniform combustion process
 without any thermal anomalies to report.

----- Reduction Parameters -----

C-Factor (Methane) : 0.04381603
 Conversion Factor : 13.100 MJ/kg 02
 Baseline O2 Reading : 20.983 %
 Baseline CO2 Reading : 0.05089 %
 Baseline CO Reading : 0.00012 %

----- Test Results -----

Peak Heat Release Rate : 233.82 kW/m2 at 409.00 secs
 Average Heat Release Rate : 161.66 kW/m2
 Average Heat Release Rate T60 : 164.92 kW/m2
 Average Heat Release Rate T180: 154.49 kW/m2
 Average Heat Release Rate T300: 144.87 kW/m2
 Total Heat Released : 74.28 MJ/m2
 Average Effective HOC : 13.44 MJ/kg
 Average Specific Ext Area : 65.55 m2/kg
 Average Mass Loss Rate: : 12.369 g/s*m2
 Entered Initial Specimen Mass : 71.40 g
 Measured Final Specimen Mass : 16.12 g
 Average CO Yield : 0.00223 kg/kg
 Average CO2 Yield : 1.44792 kg/kg
 Time to sustained Ignition : 32.62 secs

FILE: C:\CONE171\RAWDATA\010731A3.CDT

----- Test Parameters -----

Test Date : 31-Jul-01 Test Time : 01:18 p.m. Operator : Michael Smith

Test Scans : 228 scans, 3 secs/scan
 Test Length : 562.94 secs
 Sample Surface Area : 0.01000 m2
 Radiant Heat Flux : 35.0 kW/m2
 Sample Orientation : Horizontal
 Measured Exh. Flow : 0.024 m3/sec
 Orifice Plate : 57 mm
 Sample Material :
 External Oriented Strandboard
 SAMP.3

----- Test Notes -----

Pre-test Comments:

Samp.in double density alumn.pan edge control.
 Thermal absorber applied.
 Samp.wt.=74.2g,Samp.+pan wt.=77.4g.

Post-test Comments:

Samp.exhibited a uniform combustion process
 without any thermal anomalies to report.

----- Reduction Parameters -----

C-Factor (Methane) : 0.04381603
 Conversion Factor : 13.100 MJ/kg 02
 Baseline O2 Reading : 20.981 %
 Baseline CO2 Reading : 0.05175 %
 Baseline CO Reading : 0.00010 %

----- Test Results -----

Peak Heat Release Rate : 246.64 kW/m2 at 433.00 secs
 Average Heat Release Rate : 155.26 kW/m2
 Average Heat Release Rate T60 : 174.22 kW/m2
 Average Heat Release Rate T180: 158.42 kW/m2
 Average Heat Release Rate T300: 141.60 kW/m2
 Total Heat Released : 81.99 MJ/m2
 Average Effective HOC : 13.63 MJ/kg
 Average Specific Ext Area : 69.57 m2/kg
 Average Mass Loss Rate: : 12.240 g/s*m2
 Entered Initial Specimen Mass : 77.40 g
 Measured Final Specimen Mass : 17.24 g
 Average CO Yield : 0.00211 kg/kg
 Average CO2 Yield : 1.46153 kg/kg
 Time to sustained Ignition : 38.11 secs

FILE: C:\CONE171\RAWDATA\010731A4.CDT

----- Test Parameters -----

Test Date : 31-Jul-01 Test Time : 01:35 p.m. Operator : Michael Smith

Test Scans : 247 scans, 3 secs/scan
 Test Length : 621.95 secs
 Sample Surface Area : 0.01000 m2
 Radiant Heat Flux : 35.0 kW/m2
 Sample Orientation : Horizontal
 Measured Exh. Flow : 0.024 m3/sec
 Orifice Plate : 57 mm
 Sample Material :
 External 5 PLY Plywood
 SAMP.1

----- Test Notes -----

Pre-test Comments:

Samp.in double density alumn.pan edge control.
 Thermal absorber applied.
 Samp.wt.=63.6g,Samp.+pan wt.=66.6g.

Post-test Comments:

Samp.exhibited a uniform combustion process
 without any thermal anomalies to report.

----- Reduction Parameters -----

C-Factor (Methane) : 0.04381603
 Conversion Factor : 13.100 MJ/kg 02
 Baseline O2 Reading : 20.984 %
 Baseline CO2 Reading : 0.05404 %
 Baseline CO Reading : 0.00011 %

----- Test Results -----

Peak Heat Release Rate : 220.48 kW/m2 at 454.00 secs
 Average Heat Release Rate : 108.64 kW/m2
 Average Heat Release Rate T60 : 112.37 kW/m2
 Average Heat Release Rate T180: 82.65 kW/m2
 Average Heat Release Rate T300: 86.52 kW/m2
 Total Heat Released : 63.26 MJ/m2
 Average Effective HOC : 12.80 MJ/kg
 Average Specific Ext Area : 51.79 m2/kg
 Average Mass Loss Rate: : 9.555 g/s*m2
 Entered Initial Specimen Mass : 66.60 g
 Measured Final Specimen Mass : 17.17 g
 Average CO Yield : 0.00155 kg/kg
 Average CO2 Yield : 1.31432 kg/kg
 Time to sustained Ignition : 40.71 secs

FILE: C:\CONE171\RAWDATA\010731A5.CDT

----- Test Parameters -----

Test Date : 31-Jul-01 Test Time : 01:54 p.m. Operator : Michael Smith

Test Scans : 228 scans, 3 secs/scan
 Test Length : 562.37 secs
 Sample Surface Area : 0.01000 m2
 Radiant Heat Flux : 35.0 kW/m2
 Sample Orientation : Horizontal
 Measured Exh. Flow : 0.024 m3/sec
 Orifice Plate : 57 mm
 Sample Material :
 External 5 PLY Plywood
 SAMP.2

----- Test Notes -----

Pre-test Comments:
 Samp.in double density alumn.pan edge control.
 Thermal absorber applied.
 Samp.wt.=59.0g,Samp.+pan wt.=61.9g.

Post-test Comments:
 Samp.exhibited a uniform combustion process
 without any thermal anomalies to report.

----- Reduction Parameters -----

C-Factor (Methane) : 0.04381603
 Conversion Factor : 13.100 MJ/kg 02
 Baseline O2 Reading : 20.985 %
 Baseline CO2 Reading : 0.05104 %
 Baseline CO Reading : 0.00009 %

----- Test Results -----

Peak Heat Release Rate : 201.86 kW/m2 at 430.00 secs
 Average Heat Release Rate : 112.72 kW/m2
 Average Heat Release Rate T60 : 115.17 kW/m2
 Average Heat Release Rate T180: 87.06 kW/m2
 Average Heat Release Rate T300: 97.40 kW/m2
 Total Heat Released : 58.52 MJ/m2
 Average Effective HOC : 12.82 MJ/kg
 Average Specific Ext Area : 59.05 m2/kg
 Average Mass Loss Rate: : 9.897 g/s*m2
 Entered Initial Specimen Mass : 61.90 g
 Measured Final Specimen Mass : 16.21 g
 Average CO Yield : 0.00133 kg/kg
 Average CO2 Yield : 1.33092 kg/kg
 Time to sustained Ignition : 46.32 secs

FILE: C:\CONE171\RAWDATA\010731A6.CDT

----- Test Parameters -----

Test Date : 31-Jul-01 Test Time : 02:11 p.m. Operator : Michael Smith

Test Scans : 227 scans, 3 secs/scan
Test Length : 561.41 secs
Sample Surface Area : 0.01000 m2
Radiant Heat Flux : 35.0 kW/m2
Sample Orientation : Horizontal
Measured Exh. Flow : 0.024 m3/sec
Orifice Plate : 57 mm
Sample Material :
External 5 PLY Plywood
SAMP.3

----- Test Notes -----

Pre-test Comments:

Samp.in double density alumn.pan edge control.
Thermal absorber applied.
Samp.wt.=62.6g,Samp.+pan wt.=65.5g.

Post-test Comments:

Samp.exhibited a uniform combustion process
without any thermal anomalies to report.

----- Reduction Parameters -----

C-Factor (Methane) : 0.04381603
Conversion Factor : 13.100 MJ/kg 02
Baseline O2 Reading : 20.986 %
Baseline CO2 Reading : 0.05039 %
Baseline CO Reading : 0.00009 %

----- Test Results -----

Peak Heat Release Rate : 238.41 kW/m2 at 415.00 secs
Average Heat Release Rate : 124.83 kW/m2
Average Heat Release Rate T60 : 143.02 kW/m2
Average Heat Release Rate T180: 109.21 kW/m2
Average Heat Release Rate T300: 102.26 kW/m2
Total Heat Released : 63.66 MJ/m2
Average Effective HOC : 13.17 MJ/kg
Average Specific Ext Area : 56.65 m2/kg
Average Mass Loss Rate: : 10.248 g/s*m2
Entered Initial Specimen Mass : 65.50 g
Measured Final Specimen Mass : 17.16 g
Average CO Yield : 0.00183 kg/kg
Average CO2 Yield : 1.38610 kg/kg
Time to sustained Ignition : 54.23 secs

FILE: C:\CONE171\RAWDATA\010731A7.CDT

----- Test Parameters -----

Test Date : 31-Jul-01 Test Time : 02:46 p.m. Operator : Michael Smith

Test Scans : 171 scans, 3 secs/scan
 Test Length : 393.60 secs
 Sample Surface Area : 0.01000 m2
 Radiant Heat Flux : 70.0 kW/m2
 Sample Orientation : Horizontal
 Measured Exh. Flow : 0.024 m3/sec
 Orifice Plate : 57 mm
 Sample Material :
 External Oriented Strandboard
 SAMP.1

----- Test Notes -----

Pre-test Comments:

Samp.in double density alumn.pan edge control.
 Thermal absorber applied.
 Samp.wt.=72.3g,Samp.+pan wt.=75.6g.

Post-test Comments:

Samp.exhibited a uniform combustion process
 without any thermal anomalies to report.

----- Reduction Parameters -----

C-Factor (Methane) : 0.04381603
 Conversion Factor : 13.100 MJ/kg 02
 Baseline O2 Reading : 20.989 %
 Baseline CO2 Reading : 0.05890 %
 Baseline CO Reading : 0.00009 %

----- Test Results -----

Peak Heat Release Rate : 325.77 kW/m2 at 34.00 secs
 Average Heat Release Rate : 219.88 kW/m2
 Average Heat Release Rate T60 : 263.24 kW/m2
 Average Heat Release Rate T180: 223.34 kW/m2
 Average Heat Release Rate T300: 223.88 kW/m2
 Total Heat Released : 84.46 MJ/m2
 Average Effective HOC : 14.20 MJ/kg
 Average Specific Ext Area : 117.30 m2/kg
 Average Mass Loss Rate: : 16.520 g/s*m2
 Entered Initial Specimen Mass : 75.60 g
 Measured Final Specimen Mass : 16.10 g
 Average CO Yield : 0.00359 kg/kg
 Average CO2 Yield : 1.46371 kg/kg
 Time to sustained Ignition : 10.55 secs

FILE: C:\CONE171\RAWDATA\010731A8.CDT

----- Test Parameters -----

Test Date : 31-Jul-01 Test Time : 03:01 p.m. Operator : Michael Smith

Test Scans : 171 scans, 3 secs/scan
Test Length : 393.92 secs
Sample Surface Area : 0.01000 m2
Radiant Heat Flux : 70.0 kW/m2
Sample Orientation : Horizontal
Measured Exh. Flow : 0.024 m3/sec
Orifice Plate : 57 mm
Sample Material :
External Oriented Strandboard
SAMP.2

----- Test Notes -----

Pre-test Comments:

Samp.in double density alumn.pan edge control.
Thermal absorber applied.
Samp.wt.=74.3g,Samp.+pan wt.=77.5g.

Post-test Comments:

Samp.exhibited a uniform combustion process
without any thermal anomalies to report.

----- Reduction Parameters -----

C-Factor (Methane) : 0.04381603
Conversion Factor : 13.100 MJ/kg 02
Baseline O2 Reading : 20.986 %
Baseline CO2 Reading : 0.04789 %
Baseline CO Reading : 0.00009 %

----- Test Results -----

Peak Heat Release Rate : 332.89 kW/m2 at 34.00 secs
Average Heat Release Rate : 225.25 kW/m2
Average Heat Release Rate T60 : 271.41 kW/m2
Average Heat Release Rate T180: 234.63 kW/m2
Average Heat Release Rate T300: 236.61 kW/m2
Total Heat Released : 86.51 MJ/m2
Average Effective HOC : 14.20 MJ/kg
Average Specific Ext Area : 124.59 m2/kg
Average Mass Loss Rate: : 17.007 g/s*m2
Entered Initial Specimen Mass : 77.50 g
Measured Final Specimen Mass : 16.57 g
Average CO Yield : 0.00407 kg/kg
Average CO2 Yield : 1.50906 kg/kg
Time to sustained Ignition : 10.03 secs

FILE: C:\CONE171\RAWDATA\010731A8.CDT

----- Test Parameters -----

Test Date : 31-Jul-01 Test Time : 03:15 p.m. Operator : Michael Smith

Test Scans : 184 scans, 3 secs/scan
Test Length : 432.87 secs
Sample Surface Area : 0.01000 m2
Radiant Heat Flux : 70.0 kW/m2
Sample Orientation : Horizontal
Measured Exh. Flow : 0.024 m3/sec
Orifice Plate : 57 mm
Sample Material :
External Oriented Strandboard
SAMP.3

----- Test Notes -----

Pre-test Comments:

Samp.in double density alumn.pan edge control.
Thermal absorber applied.
Samp.wt.=82.2g,Samp.+pan wt.=85.4g.

Post-test Comments:

Samp.exhibited a uniform combustion process
without any thermal anomalies to report.

----- Reduction Parameters -----

C-Factor (Methane) : 0.04381603
Conversion Factor : 13.100 MJ/kg 02
Baseline O2 Reading : 20.986 %
Baseline CO2 Reading : 0.04896 %
Baseline CO Reading : 0.00009 %

----- Test Results -----

Peak Heat Release Rate : 328.92 kW/m2 at 40.00 secs
Average Heat Release Rate : 225.23 kW/m2
Average Heat Release Rate T60 : 265.81 kW/m2
Average Heat Release Rate T180: 236.29 kW/m2
Average Heat Release Rate T300: 231.97 kW/m2
Total Heat Released : 95.28 MJ/m2
Average Effective HOC : 14.16 MJ/kg
Average Specific Ext Area : 129.81 m2/kg
Average Mass Loss Rate: : 17.266 g/s*m2
Entered Initial Specimen Mass : 85.40 g
Measured Final Specimen Mass : 18.12 g
Average CO Yield : 0.00408 kg/kg
Average CO2 Yield : 1.49875 kg/kg
Time to sustained Ignition : 11.20 secs

FILE: C:\CONE171\RAWDATA\010731B1.CDT

----- Test Parameters -----

Test Date : 31-Jul-01 Test Time : 03:34 p.m. Operator : Michael Smith

Test Scans : 159 scans, 3 secs/scan
Test Length : 355.86 secs
Sample Surface Area : 0.01000 m2
Radiant Heat Flux : 70.0 kW/m2
Sample Orientation : Horizontal
Measured Exh. Flow : 0.024 m3/sec
Orifice Plate : 57 mm
Sample Material :
External 5 PLY Plywood
SAMP.1

----- Test Notes -----

Pre-test Comments:
Samp.in double density alumn.pan edge control.
Thermal absorber applied.
Samp.wt.=58.0g,Samp.+pan wt.=60.9g.

Post-test Comments:
Samp.exhibited a uniform combustion process
without any thermal anomalies to report.

----- Reduction Parameters -----

C-Factor (Methane) : 0.04381603
Conversion Factor : 13.100 MJ/kg 02
Baseline O2 Reading : 20.986 %
Baseline CO2 Reading : 0.04953 %
Baseline CO Reading : 0.00008 %

----- Test Results -----

Peak Heat Release Rate : 257.48 kW/m2 at 49.00 secs
Average Heat Release Rate : 167.08 kW/m2
Average Heat Release Rate T60 : 174.59 kW/m2
Average Heat Release Rate T180: 159.94 kW/m2
Average Heat Release Rate T300: 178.10 kW/m2
Total Heat Released : 59.15 MJ/m2
Average Effective HOC : 13.04 MJ/kg
Average Specific Ext Area : 105.84 m2/kg
Average Mass Loss Rate: : 14.742 g/s*m2
Entered Initial Specimen Mass : 60.90 g
Measured Final Specimen Mass : 15.54 g
Average CO Yield : 0.00235 kg/kg
Average CO2 Yield : 1.37760 kg/kg
Time to sustained Ignition : 6.73 secs

FILE: C:\CONE171\RAWDATA\010731B2.CDT

----- Test Parameters -----

Test Date : 31-Jul-01 Test Time : 03:51 p.m. Operator : Michael Smith

Test Scans : 169 scans, 3 secs/scan
 Test Length : 387.58 secs
 Sample Surface Area : 0.01000 m2
 Radiant Heat Flux : 70.0 kW/m2
 Sample Orientation : Horizontal
 Measured Exh. Flow : 0.024 m3/sec
 Orifice Plate : 57 mm
 Sample Material :
 External 5 PLY Plywood
 SAMP.2

----- Test Notes -----

Pre-test Comments:
 Samp.in double density alumn.pan edge control.
 Thermal absorber applied.
 Samp.wt.=60.3g,Samp.+pan wt.=63.2g.

Post-test Comments:
 Samp.exhibited a uniform combustion process
 without any thermal anomalies to report.

----- Reduction Parameters -----

C-Factor (Methane) : 0.04381603
 Conversion Factor : 13.100 MJ/kg 02
 Baseline O2 Reading : 20.987 %
 Baseline CO2 Reading : 0.04982 %
 Baseline CO Reading : 0.00009 %

----- Test Results -----

Peak Heat Release Rate : 262.58 kW/m2 at 25.00 secs
 Average Heat Release Rate : 169.23 kW/m2
 Average Heat Release Rate T60 : 169.96 kW/m2
 Average Heat Release Rate T180: 149.30 kW/m2
 Average Heat Release Rate T300: 176.07 kW/m2
 Total Heat Released : 64.48 MJ/m2
 Average Effective HOC : 13.56 MJ/kg
 Average Specific Ext Area : 141.90 m2/kg
 Average Mass Loss Rate: : 13.859 g/s*m2
 Entered Initial Specimen Mass : 63.20 g
 Measured Final Specimen Mass : 15.66 g
 Average CO Yield : 0.00335 kg/kg
 Average CO2 Yield : 1.41203 kg/kg
 Time to sustained Ignition : 9.76 secs

FILE: C:\CONE171\RAWDATA\010731B3.CDT

----- Test Parameters -----

Test Date : 31-Jul-01 Test Time : 04:04 p.m. Operator : Michael Smith

Test Scans : 179 scans, 3 secs/scan
 Test Length : 417.46 secs
 Sample Surface Area : 0.01000 m2
 Radiant Heat Flux : 70.0 kW/m2
 Sample Orientation : Horizontal
 Measured Exh. Flow : 0.024 m3/sec
 Orifice Plate : 57 mm
 Sample Material :
 External 5 PLY Plywood
 SAMP.3

----- Test Notes -----

Pre-test Comments:

Samp.in double density alumn.pan edge control.
 Thermal absorber applied.
 Samp.wt.=65.0g,Samp.+pan wt.=67.8g.

Post-test Comments:

Samp.exhibited a uniform combustion process
 without any thermal anomalies to report.

----- Reduction Parameters -----

C-Factor (Methane) : 0.04381603
 Conversion Factor : 13.100 MJ/kg 02
 Baseline O2 Reading : 20.988 %
 Baseline CO2 Reading : 0.05011 %
 Baseline CO Reading : 0.00009 %

----- Test Results -----

Peak Heat Release Rate : 240.95 kW/m2 at 22.00 secs
 Average Heat Release Rate : 168.73 kW/m2
 Average Heat Release Rate T60 : 147.92 kW/m2
 Average Heat Release Rate T180: 161.98 kW/m2
 Average Heat Release Rate T300: 185.50 kW/m2
 Total Heat Released : 69.85 MJ/m2
 Average Effective HOC : 13.73 MJ/kg
 Average Specific Ext Area : 143.74 m2/kg
 Average Mass Loss Rate: : 14.741 g/s*m2
 Entered Initial Specimen Mass : 67.80 g
 Measured Final Specimen Mass : 16.91 g
 Average CO Yield : 0.00461 kg/kg
 Average CO2 Yield : 1.39783 kg/kg
 Time to sustained Ignition : 6.69 secs